

**SELF-LOCALIZATION OF TARGET NODES USING OPPORTUNISTIC
COMMUNICATION WITH REFERENCE NODES, STATISTICAL
TIME-OF-ARRIVAL, GRID METHOD, LINEAR MATRIX INEQUALITY AND
CENTER-OF-GRAVITY**

by

Abhishek Arunkumar Kulkarni

A Thesis submitted to the Graduate Faculty of
Auburn University
in Partial Fulfillment of the
Requirements for the Degree of
Master of Science

Auburn, Alabama
May 7, 2016

Approved by

Alvin S. Lim, Co-Chair, Professor of Computer Science and Software Engineering
Shiwen Mao, Co-Chair, Professor of Electrical and Computer Engineering
Thaddeus Roppel, Associate Professor of Electrical and Computer Engineering

ABSTRACT

Self-localization of mobile nodes is an important problem because many useful mobile applications will become feasible once accurate position information is available. Generally, existing methods for obtaining accurate location information require either sophisticated hardware (e.g. Global Positioning System (GPS), Ultra-Wideband (UWB), ultrasounds transceiver) or dedicated infrastructures (e.g. GSM, WLAN). We address this problem using a different approach that requires no special hardware or infrastructure support. The main concept adapted to solve this problem is: localization can be performed and improved by means of cooperative and opportunistic data exchanges among mobile nodes. Consider a GPS-denied target node with no position information that communicates opportunistically with a number of in-range mobile peer nodes with some positioning capabilities. The data exchanges between the target node and the peer nodes will then be used by the target node to refine its position estimation using a combination of these algorithms: Statistical Time-of-Arrival (TOA), Linear Matrix Inequalities (LMI), barycentric algorithms, Grid Method and Center of Gravity (COG) techniques. Approximate ranging using Statistical TOA method using Bhattacharyya Distance enables the LMI, Grid Method, barycentric algorithms and Center of Gravity(COG) technique to improve position accuracy. To investigate the performance of such an opportunistic localization algorithm, we define a simple model that describes the opportunistic interactions between nodes and then we run several computer simulations to analyze the effect of the ranging error on the positioning of the target node. Along with the simulation model we have conducted the experiments with real-world data to measure the performance of the techniques in the real-world. The results generated from both simulation and real-world data show that opportunistic interactions can actually improve self-localization accuracy, where the position estimation error is about 2 m or less in many different scenarios.

ACKNOWLEDGEMENTS

I would like to express my appreciation to Dr. Lim for the guidance he has provided throughout my study at Auburn. I would also like to express my gratitude to the advisory committee members, Dr. Shiwen Mao and Dr. Thaddeus Roppel.

I would also like to thank several fellow students including Song Gao and Amogh Kashyap for their significant contributions to this research.

Above all, I would like to thank my parents who helped me come to U.S. and pursue graduate study at Auburn.

Style manual or journal used Journal of Approximation Theory (together with the style known as "aums"). Bibliography follows van Leunen's *A handbook for Scholars*.

Computer Software used The document preparation package $\text{T}_{\text{E}}\text{X}$ (specifically $\text{L}^{\text{A}}\text{T}_{\text{E}}\text{X}$) together with the departmental style-file aums.sty.

Table of Contents

Abstract	ii
Acknowledgements	iii
List of Figures	viii
List of Tables	xi
1 INTRODUCTION	1
2 MOTIVATIONS AND APPLICATIONS	5
2.1 Motivation	5
2.2 Applications	6
2.2.1 Hospitals, Warehouses and University Campus	6
2.2.2 Indoor Tracking of Firefighters	6
2.2.3 Localization of Wireless Sensor Network	7
2.2.4 Airports and Subway Stations	7
2.2.5 Robot localization	7
2.2.6 Museums	8
2.2.7 Targeted Advertising and Warning Alerts	8
3 RELATED WORK	10
3.1 Ranging Technique	10
3.2 Navigation Using Ultra Wideband (UWB)	12
3.3 Navigation using Received Signal Strength Indicator (RSSI)	13
3.4 Navigation using Time-of-Arrival (TOA) and Time-difference-of-Arrival (TDoA)	14
3.5 Navigation using Angle-of-Arrival (AoA)	15
4 PROBLEM STATEMENT	16
4.1 Problem Statement	16

4.2	Conceptual Approach	17
4.2.1	Assumptions and Goals	18
4.2.2	Time-of-Arrival Ranging Technique	18
4.2.3	Linear Matrix Inequality Technique	19
4.2.4	Grid Method	19
4.2.5	Barycentric Algorithm	20
4.2.6	Center-of-Gravity Technique	20
5	DESIGN AND METHODS	21
5.1	Ranging Model	21
5.2	Ranging techniques	22
5.2.1	Euclidean Time-of-Arrival Ranging Method	22
5.2.2	Statistical Time-of-Arrival Ranging Method	23
5.3	Self-Localization of Target Node	25
5.3.1	Raw LMI Estimation	26
5.3.2	Self-Localization using Linear Matrix Inequality and Barycentric Algorithm	27
5.3.3	Self-localization using Linear Matrix Inequality and Center of Gravity Technique	28
5.3.4	Self-positioning using Grid Method Technique	29
6	IMPLEMENTATION	31
6.1	Simulation Setup and Implementation	31
6.2	Reference Case	31
6.2.1	Linear Matrix Inequality with Barycentric Algorithm	31
6.2.2	Linear Matrix Inequality with Center Of Gravity Technique	32
6.2.3	Varying Time-of-Arrival Induced Error	32
6.2.4	Random Waypoint Mobility Model Analysis	33
6.2.5	Firefighter Mobility Model Analysis	34
6.3	Real-World Model Specifications	35

7	PERFORMANCE EVALUATION	36
7.1	Simulation Result	36
7.2	Accuracy of reference case	36
7.2.1	Linear matrix Inequality with Barycentric Algorithm	36
7.2.2	Linear Matrix Inequality with Center Of Gravity Technique	40
7.2.3	LMI with varying Euclidean Time-Of-Arrival Distance Error	41
7.3	Simulation Results of Mobility Models	42
7.3.1	Linear Matrix Inequality with Random Waypoint Mobility Model	43
7.3.2	Linear Matrix Inequality with Firefighter Mobility Model	44
7.3.3	Grid Method with Center-of-Gravity	49
7.3.4	Comparison of Linear Matrix Inequality Technique and Grid Method for Simulation Model	54
7.3.5	Comparison of Linear Matrix Inequality Technique and Grid Method for Real World Data	56
8	CONCLUSION	69
8.1	Conclusion	69
8.2	Future Work	71

List of Figures

5.1	(a) Histogram of RTT samples for reference node at 10m and (b) Probability density estimate of RTT samples for reference node at 10m	24
5.2	Probability density estimate of RTT samples for reference node at 20m	25
5.3	Probability density estimate of RTT samples for reference node at 30m	25
5.4	Raw Position Estimation using only Linear Matrix Inequality	27
5.5	Position Estimation using Linear Matrix Inequality and Barycentric Algorithm	28
5.6	Plot of all the grid points in the intersection area including the reference node and real target node positions	30
7.1	LMI-only Error Estimation	37
7.2	LMI+barycenter Error Estimation	38
7.3	Error comparison Between LMI-only and LMI+barycenter	39
7.4	LMI-Only Estimation Error for Varying Node Range	40
7.5	LMI+Barycenter Estimation Error for Varying Node Range	41
7.6	LMI+Barycenter Estimation for actual devices	42
7.7	LMI+Center Of Gravity Estimation	43
7.8	LMI+COG with Varying TOA error	44
7.9	LMI with RWMM and Varying Pause time	45
7.10	LMI with Firefighter Mobility Model and COG	46
7.11	Firefighter mobility with LMI and COG along with different Target node positions	47
7.12	Firefighter mobility with LMI and COG along with different Target node positions and larger communication range	48
7.13	MATLAB Map of Shelby Foyer (Auburn University) including all the peer nodes, Real Target node and Estimated Target node Positions	49

7.14	The Indoor map of Shelby Foyer (Auburn University) including all the peer nodes, Target node and estimated target node positions	50
7.15	MatLab Map of Shelby Center Hallway (Auburn University) including all the peer nodes, Real Target node and Estimated Target node Positions	51
7.16	The Indoor map of Shelby Center Hallway (Auburn University) including all the peer nodes, Target node and estimated target node positions	52
7.17	Plot of reference node position, Real Target node and Target node position estimated from Grid and LMI method	53
7.18	The difference between normal circle communication model and Donut circle Communication model	54
7.19	Plot of reference node positions with donuts, real target node and grid points	55
7.20	Plot of reference node positions, real target node position and target node position estimated from Grid and LMI methods	56
7.21	Plot of reference nodes with donuts and Grid points for different intersection areas	57
7.22	Plot of Reference node positions, Real target node and estimated target node position from Grid and LMI method for Auburn University Shelby Hallway	58
7.23	Plot of reference node positions, real Target node position and estimated target node position from Grid and LMI methods for Auburn University Shelby Foyer	59
7.24	Plot of reference node positions, real Target node position and estimated target node position from Grid and LMI methods for Auburn University Hallway and multiple rooms	60
7.25	Plot of target node location error comparison between LMI and Grid method with 20% induced TOA distance error.	61
7.26	Plot of target node location error comparison between LMI and Grid method with 50% induced TOA distance error.	62
7.27	Plot of target node location error comparison between LMI and Grid method with 80% induced TOA distance error.	63
7.28	Plot of target node location error comparison between LMI and Grid method with 100% induced TOA distance error.	64
7.29	Plot of target node location error comparison between LMI and Grid method for Statistical TOA data for Auburn University Foy Hall Main Floor	65
7.30	Plot of target node location error comparison between LMI and Grid method for Statistical TOA data for Auburn University Shelby center hallway and multiple rooms.	66

7.31 Plot of target node location error comparison between LMI and Grid method for Statistical TOA data for Auburn University Shelby center hallway and multiple rooms. . . 67

7.32 Plot of target node location error comparison between LMI and Grid method for Statistical TOA data for Auburn University Broun hall Second floor. 68

List of Tables

6.1	Reference case parameters	31
6.2	Firefighter Mobility Model parameters	35
6.3	Real-World Model Specification	35
7.1	The co-ordinates are of the peer nodes and the TOA distances are obtained from Statistical TOA technique for Auburn university Shelby Foyer	47
7.2	The co-ordinates are of the peer nodes and the TOA distances are obtained from Statistical TOA technique at Auburn University Shelby Center Hallway	48
7.3	Table representing the Statistical TOA data for Auburn University Shelby Center hallway with Peer Reference node co-ordinates	52
7.4	Table representing the Statistical TOA data for Auburn University Foy Hall Main Floor with Peer Reference node co-ordinates	57
7.5	Table representing the Statistical TOA data for Multiple rooms of Auburn University Shelby Center hallway and multiple rooms with Peer Reference node co-ordinates	59
7.6	Table representing the Statistical TOA data for Multiple rooms of Auburn University Shelby Center with Peer Reference node co-ordinates	60
7.7	Table representing the Statistical TOA data for Multiple rooms of Auburn University Shelby Center with Peer Reference node co-ordinates	62

Chapter 1

INTRODUCTION

Introduction

In the year 2000 the Defense Department removed the purposeful degradation of the accuracy of Global Positioning System (GPS) which increased the accuracy of GPS ten times compared to the older version available to civilians [42]. This event encouraged the industry to develop devices for monitoring and tracking various objects. In the next decade we have seen an extensive usage of GPS devices and with the increasing usage of the GPS devices the demand for better accuracy increased as well. The current GPS devices are far more accurate than its predecessors. But one of the main drawbacks of GPS is that the satellite signals cannot penetrate through buildings, dense forests, urban canyons etc. This restricts the usage of GPS strictly to outdoor environments where there is a clear line-of-sight signal from the satellites. There were numerous research works being carried out to solve this problem and develop a new technology which can provide accurate monitoring and tracking for indoor environment [29, 2, 9, 26]. But due to the lack of technological support during these early researches it was not feasible to produce acceptable accuracy. The importance of monitoring and tracking of devices gained speed again during the early years of this decade with the support from technological advancement in the industry.

Wireless ad-hoc network is a computer network which communicates data without utilizing any infrastructure or wires compared to other computer networks. The nodes in ad-hoc mode can communicate and maintain a network on their own. The nodes in ad-hoc networks are responsible for delivering data to other nodes. Ad-hoc network can also utilize flooding protocol to forward the data through the network, but there are many routing protocols which are more efficient than flooding routing protocol such as proactive routing, location-based routing, hybrid routing etc. The maintenance of ad-hoc network is fairly simple and flexible compared to other networks which

involve infrastructures [52]. The flexibility in maintenance of ad hoc network is the reason we chose ad hoc network as our mobile networking system.

In mobile and ad-hoc networks, the knowledge of the position and trajectory of the nodes represents an important information that can be exploited for many different purposes, such as communication protocols optimization, path planning, and cooperative task design. The accuracy of localization estimation is strictly related to the environment and the technology used by the devices to localize themselves. An inexpensive and widespread technology that utilizes Received Signal Strength Indicator (RSSI) gives poor localization performance [57], while more expensive hardware used in comparing the Time-of-Arrival (TOA) of radio signals [48] can provide better accuracy. However, special localization hardware will drive up the cost of mobile devices whereas localization methods that use low-cost Commercial off-the-shelf hardware that provide similar accuracy will be more viable alternatives.

Accurate localization or tracking of wireless devices is a crucial requirement for many emerging location-aware systems. Fields of applications include search and rescue, medical care, intelligent transportation, location-based billing, security, home automation, industrial monitoring and control, location-assisted gaming, and social networking. The main trend now is toward the integration of heterogeneous technologies to ensure global coverage and high accuracy in all possible scenarios, leading to a seamless localization system available anywhere anytime. The satellite-based navigation (GPS) is well consolidated for open sky scenarios but localization in harsh environments (e.g., indoor or in urban areas) is still an open issue that requires a new technology which utilizes the wireless network to provide self-localization. In order to fulfil these needs of the modern world, we constructed a new method of localization based on opportunistic data exchanges.

Most of the literature on localization focus on systems and algorithms explicitly designed to provide localization functionality to nodes such as GPS-equipped devices, whereas we investigate how localization can be obtained through opportunistic interactions in systems that may not be designed with such a sophisticated service or in GPS-denied environments. An example is that of a tourist traveling on a highway who may desire to estimate his position by opportunistically

exchanging data with the passing vehicles that are equipped with GPS localization or other sophisticated positioning systems. Self-localization can be of much importance in driverless cars which will soon become a part of our world [13]. Also, in the current world where everyone has a handheld smartphones (equipped with GPS), a person with a normal mobile phone (GPS-less devices) will be able to self-locate himself by exchanging data opportunistically with the neighboring nodes.

Opportunistic localization consists of communication between target node and reference peer nodes to exchange necessary information and obtain the position of the target node. The mode of communication is performed using IEEE 802.11g WiFi protocol at 2.4 GHz and 5.9 GHz frequencies. The ranging technique to calculate the distance between target node and the reference peer nodes is accomplished by using Time-of-Arrival (TOA). There are many ranging techniques other than Time-of-Arrival (TOA) such as Received Signal Strength Indicator (RSSI), Angle-of-Arrival (AOA), Time-Difference-of-Arrival (TDOA) etc. [5] But we chose Time-of-Arrival (TOA) as it is more accurate and reliable than Received Signal Strength Indicator (RSSI) and less expensive than Angle-of-Arrival (AOA). We obtain Time-of-Arrival (TOA) data from each reference peer node by collecting the Round-Trip-Time (RTT) at driver layer of the FreeBSD kernel and matching them statistically our database which converts the RTT times into distance between the Target node and reference peer nodes. [51]

Once the distance is obtained from the TOA technique, along with the co-ordinates of reference peer nodes we can calculate the position of the target node using Linear Matrix Inequality (LMI) [43] and Grid method. Linear Matrix Inequality (LMI) is a mathematical technique to solve optimization problems and is extensively used in System and Control theory of mechanical engineering, but it can also be used to solve localization as we proved with our solution. Another technique used to solve the localization problem is Grid method which involves collecting a cluster of grid points in the intersection area of all the reference peer nodes which includes the position of target node. This technique is called multilateration [50] and is used by Global Positioning system (GPS) and many other navigation techniques. After performing Linear Matrix Inequality (LMI)

and Grid method we obtain the position co-ordinates of target node with an accuracy of less than 2 meters. In order to refine the results obtained from Linear Matrix Inequality (LMI) and Grid method we perform Center-of-Gravity (COG) technique to improve the accuracy to less than a meter.

The remainder of the thesis is structured as follows. In Chapter 2 we formerly address the background information about the related research work to our technology for localization and ranging. In Chapter 3 we describe the motivations and applications for our work. In Chapter 4 we explains the problem statement of our research work. The details of design and methods utilized for our research is explained in Chapter 5. Chapter 6 explains the implementation of our research with simulation setup. In Chapter 7 we evaluate the performance of our technology with simulation and real-world results. Finally, Chapter 8 draws the conclusion and states some future work of the research.

Chapter 2

MOTIVATIONS AND APPLICATIONS

In this chapter we will discuss the motivations for our localization technology as well as its applications.

2.1 Motivation

Although indoor tracking has been an important research area since early 2000s, it has been difficult to develop a system with required accuracy. Indoor tracking using Global Positioning System (GPS) does not work as the GPS satellite signals cannot reach indoor environment. As a result, the accuracy of the position is very poor. Also, other research techniques like Ultra wideband (UWB) produce acceptable accuracy but it is very expensive to deploy these devices. Other techniques like Received Signal Strength indicator (RSSI), although very easy to develop and maintain produces poor accuracy and is unreliable in most cases. This motivated us to develop a new technique to solve the indoor tracking system which can provide better accuracy and cost-effective to deploy in large scale. We propose four methods which work together to produce indoor tracking with an acceptable accuracy. First, we propose using Time-of-Arrival (TOA) ranging method at the driver level of the software kernel to generate Round-Trip-Time (RTT) between the Target node and the reference peer nodes. Secondly, we utilize these RTT times and match it with our database of RTT times using Statistical methods such as Bhattacharyya Distance to obtain the distance between Target node and reference peer nodes. Third, we use these distances along with the positions of reference peer nodes to generate the Target node position using techniques like Linear Matrix inequality (LMI) and Grid method. Lastly, we improve the accuracy of the positions obtained by performing Center-of-Gravity (COG) technique.

2.2 Applications

Indoor tracking system can support a wide range of applications such indoor tracking of objects inside a hospital, mall, university campus buildings, automobile plant etc. It can also provide tracking of personnel inside the buildings for firefighters as they work in extreme conditions with vision being close to nil. The system can also provide navigation and directions in complex buildings and ease the pain of being lost. Some of the important applications are explained in the following sections.

2.2.1 Hospitals, Warehouses and University Campus

Hospitals can be complex environment to navigate and find the exact room for an appointment. It can be almost impossible to find a room without seeking any assistance from the hospital reception. This problem can be solved by our indoor navigation system which can provide directions to a particular room. Similar to hospital environment, university campus can be difficult to navigate. Most of the time students miss their classes or arrive late due to being lost searching for a particular building or room. Our technology can be deployed in handheld devices so that each and every person on campus can navigate easily without getting lost. Our technology can also be applied to object along with human beings. In a warehouse it is very easy to misplace any of the equipment and it could become a daunting task to locate it inside such a huge environment. In order to solve this we can deploy our technology can attach devices to important equipment so that we can never lose track of that object.

2.2.2 Indoor Tracking of Firefighters

Firefighters work in one of most dangerous environment and put their lives on the line to save others. A fire scene usually consists of a lot of chaos and it could be very easy for a firefighter to get indulged inside the building in fighting fire or saving life and lose track of his teammates. It could be very difficult to navigate inside the building as the vision usually will be almost nil along with the chaos going on the scene. So, firefighters get lost inside the building more than we

can imagine. Our technology can provide a solution to this critical problem by providing a device which is capable of tracking all the firefighters on the scene. This way the Chief-in-Office on the scene can keep track of all the firefighters and if anyone of them loses track of their location, it would be easy to track the location and rescue them in time to save their lives.

2.2.3 Localization of Wireless Sensor Network

Wireless sensor network is distributed network of sensors in a spatial area deployed to measure environmental parameters such as temperature, pressure, humidity etc. These sensors also communicate and send the messages to a data center [53]. Locating each sensor in a large area can be difficult and would require a lot of manual labor. Our technology can provide a tracking system to track all the sensors and provide accurate positions of each sensors without much work. It would be easy to manage the working of all the sensors and provide assistance if any of the sensor goes burst.

2.2.4 Airports and Subway Stations

Airports and subway stations can be a very complex environment to navigate. Usually there is a time limit in order to catch your flight or a train, so you need to find the right flight gate or the right train to board for your destination. This task can be very daunting and needs a better solution in order to make everything easy for all the passengers to navigate around these complex buildings. Our indoor navigation system can provide simple directions for navigating inside these buildings for each individual depending on their flight gate or train platform. This reduces the anxiety and pain of being lost inside complex environments like airports or subway stations.

2.2.5 Robot localization

Robot localization is the robot's ability to find its position within the frame of reference. Localization is an important aspect of robotics and essential for autonomous movement of the robot to its destination. Path finding and mapping is actually an extension of localization and are

very essential for robot movement to any destination. the robot localization can be categorized into three groups as Global navigation, Local navigation and Personal navigation [11]. Among these three robot localization categories our indoor tracking system can be useful in Global and Local Navigation as these two navigation types require human-interaction or with other robots. Our technique is based on opportunistic communication between the nodes so it cannot be applied to personal navigation as in this type the robot is alone and does not interact with anything to navigate around the referenced area.

2.2.6 Museums

Our indoor navigation technology can transform each individual mobile device into a interactive tour guide for a museum. It can provide easy step-by-step navigation guidance along with information of each art according to the location of the individual. The system can also help to manage the database of the museum in addition or deletion of art in a easy and effective way. Visitors can easily obtain all the information they need by just a clicking on their mobile device. Our technology can also help the museum maintenance team to analyse different aspects such as visitor interests, behavior etc.

2.2.7 Targeted Advertising and Warning Alerts

Targeted advertising is a type of advertising to consumers depending on various traits such as behavior, demographics etc. Targeted advertising has gained a lot of importance in this decade and is currently used by many advertising companies to reach appropriate consumers in order to raise sales. These also help the consumer to get advertises which are more personalized to them compared to previous technique of flooding advertises to all consumers. Indoor navigation system can help in targeted advertising by providing the locations of all the consumers such as inside a mall. This way each shop can send their personalized advertising to their consumer when they are near the shop or entering the shop. This method will reduce a lot of advertising boards which are placed inside the shop in order to attract customers. Also, with the help of our indoor navigation

system we can send warning alerts to individuals in the area with danger. For example, if a building is on fire and the fire department want to send warning messages to alert all the individuals around the area then it can be possible by sending messages to all them based on location. This method also helps in containing the chaos to a restricted area and also provide guidance to avoid certain areas.

Chapter 3

RELATED WORK

3.1 Ranging Technique

Self-localization problem has been investigated by many researchers as indicated in a number of papers. Most common localization methods consists of measuring the power of the received RF signal (RSSI), the Time of Arrival (ToA) or the Angle of Arrival (AoA) of the RF signals from the beacons. In this way, every node estimates a set of distances from the beacons and, then, estimates its position by means of lateration and triangulation techniques [38], [37] or by using statistical estimation methods [31]. Overviews of localization techniques based on RSSI and ToA measurements can be found in [32], [39], and [24]. Multi-step localization techniques, which involve a number of successive refinement phases, have been proposed by Savarese [36] and Savvides [37]. Other solutions leveraging on specialized and complex hardware and infrastructure are given in [48]. When nodes (either static or mobile) can detect each other, then it is possible to devise cooperative position estimate techniques, which are very well studied in robotics. In [17] the authors utilize Markov localization for self-localizing nodes and, then, probabilistic methods to synchronize the robot's estimate when they have a contact. Collective localization based on a distributed Kalman Filter is proposed in [35], whereas an anchor-free approach where robots infer their position estimate on the basis of the only information exchanged among them is proposed in [23].

In [12] Doherty et al. pioneered the use of semidefinite programming (SDP) methods in the localization problem. The problem is considered as a bounding problem containing several convex geometric constraints mathematically represented as linear matrix inequalities (LMI). The mechanism proposed in this paper is based on this approach, taking into account the estimation errors and introducing a barycentric improvement over time. The Centroid localization method

[8] is developed to estimate the user's location by computing the barycenter of all the positions received from those fixed beacon nodes. To find the optimum deployment of those beacon nodes for a given application may consume a lot of labor. In the APIT method [22], a user chooses three beacon nodes around him as the triangle vertex point and uses the APIT algorithm to test if he is lying in the triangle. If the APIT test can be passed, i.e., at least one node's signal is becoming the barycenter of the triangle and will be taken as the location estimation of the user. Continuously, three other nodes will be chosen to face the APIT test again. If the new test can also be passed, the barycenter of the intersection of the triangles will be used. By analogy, the user will repeat this APIT test until all combinations are exhausted or the satisfying accuracy is achieved. It is noticeable that since the APIT test is used under the condition of static beacon nodes, accomplishing it is still not an easy thing. Additionally, the APIT test may fail in less than 14% of the cases [22].

There are many other research works which jointly solve the time synchronization and localization problems. For instance, Enlightness [4] relies on the availability of beacon nodes (at least 5% of the nodes) providing absolute time and space information, like the GPS in outdoor environments. Enlightness combines recursive positioning estimation [1] with a clock offset estimation scheme based on the measure of beacon packet delays and time-stamps.

In [15], an advanced integration of 802.11b equipments and Inertial Navigation System (INS) is used to enhance the performance of the indoor positioning system. As a result, a system performance close to the meter accuracy can be achieved with a low density of access points in the environment, provided that users carry inexpensive INS equipment.

In [45], the author presents a novel deep learning based indoor fingerprinting system using Channel State Information (CSI), which is termed DeepFi. Based on three hypotheses on CSI, the DeepFi system architecture includes an off-line training phase and an on-line localization phase. Moreover, a greedy learning algorithm is used to train the weights layer-by-layer to reduce complexity. In the on-line localization phase, we use a probabilistic method based on the radial basis function to obtain the estimated location. Experimental results are presented to confirm that

DeepFi can effectively reduce location error compared with three existing methods in two representative indoor environments. In [44] the author proposes PhaseFi, a fingerprinting system for indoor localization with calibrated channel state information (CSI) phase information. In PhaseFi, the raw phase information is first extracted from the multiple antennas and multiple subcarriers of the IEEE 802.11n network interface card (NIC) by accessing the modified driver. In [46], the author proposes DeepFi, a fingerprinting system for indoor localization with calibrated channel state information (CSI) phase information. In this paper experimental results are presented to confirm that DeepFi can effectively reduce location error compared with three existing methods in two representative indoor environments.

In paper [47], we can find a novel cooperative localization scheme exploiting mobility in the indoor environment. The problem is formulated as a semidefinite program (SDP) using Linear Matrix Inequality (LMI). Simulation results in this paper confirm that both the mean error and variance can be effectively reduced by exploiting IMU data and Kalman filter.

3.2 Navigation Using Ultra Wideband (UWB)

In [40], they propose a indoor navigation system using Ultra wideband (UWB) transmitter and receiver for communication between the nodes. They utilize Time Difference of Arrival (TDOA) technique to estimate the distance between the nodes. The main application for this system is Mobile Robot (MR) navigation and their controlled experiment results obtained an accuracy of 20 cm. Another research technique on Ultra wideband based indoor navigation is proposed in [41]. Here the author proposes an indoor navigation system using UWB-IR technique and the indoor environment is divided in to multiple cells in order to reduce the range of communication. UWB-IR technique sends out very narrow pulses which helps in differentiating the first pulse (Line-of-Sight) and the multi-path pulses. Time difference of Arrival (TDOA) technique is used to obtain the localization of target node with accuracy of 15 cm. A similar research technology using UWB developed for Mobile Robot (MR) in indoor environment is proposed in [20]. This proposes the use of PulseOn device which is a commercial UWB localization system and a GPS

receiver mounted on the Mobile Robot (MR) for indoor navigation. they obtained good results for both indoor as well as outdoor environment but this technology cannot be considered as the UWB indoor navigation technology because the robot navigates using odometer and a laser sensor. In [21], the research technology proposes a indoor navigation system by combining Ultra wideband (UWB) and inertial navigation to enhance the accuracy of personal localization called as Hybrid positioning system including sensor node, gateway and server. Experimentation results show that the hybrid algorithm not only takes advantage of UWB location coordinates to correct step length, heading and drift of DR, along with decreasing the error up to 45% compared to stand-alone UWB techniques. In [60], the indoor navigation system is designed using inertial measurement unit (IMU) and ultra wideband (UWB) localization system similar to [21]. This system is very bulky and the size is comparable to a standard backpack as seen from some of the figures in the research paper. The accuracy of the device is good as UWB provides better accuracy than normal radio signals but it comes with a cost and makes the entire device expensive.

3.3 Navigation using Received Signal Strength Indicator (RSSI)

In [30], the author proposes a Wireless localization technique for sensor network using RSSI and LQI. They perform two types of experiments which are Recursive Bayesian- RSSI-LQI (RB-RSSI-LQI) and Maximum a posteriori-RSSI-LQI (MAP-RSSI-LQI) and evaluate the accuracy comparing with the mean RSSI accuracy. the technique provides better accuracy than Mean-RSSI technique but still the accuracy is not reliable. In [54], we can find the characteristics and details about the Received Signal Strength Indicator (RSSI) technique. The experiments involve time-domain as well as frequency-domain studies. In [55] we can see a personnel position system for mine workers in a coal mine based on Received Signal Strength indicator (RSSI) technique. The paper uses the mean-RSSI of the signal to estimate the distance between nodes.

3.4 Navigation using Time-of-Arrival (TOA) and Time-difference-of-Arrival (TDoA)

In [18], they propose a localization system using IEEE 802.11 b/g timestamps to collect Time-of-Flight (ToF). Using these Time-of-Flight (ToF) samples they calculate the Time-Difference-of-Arrival (TDoA) to obtain the distance between the nodes for localization. In this paper they also discuss the histograms of TDoA samples for calculating the distance between nodes. In [16], we can see an intelligent Time-of-Arrival (TOA) technique for vehicular navigation system which takes into account the driver driving data as well as the traffic flow of the road. These data collected over time are used to make the system learn and evolve to develop better results. In this paper the author has successfully presented a new Time-of-Arrival (TOA) technique to provide better accuracy for vehicular navigation system. In [14], we can see details about Angle-of-Arrival (AoA) or also known as Direction-of-Arrival (DoA) technique to obtain the range between target node and the reference peer nodes. The paper also proposes the use Time-Difference-of-Arrival (TDoA) technique along with using the Fang's and Chan's method of solving hyperbolic equations to obtain the the position location of a node. Another Localization system using Time-Difference-of-Arrival (TDoA) ranging technique for wireless sensor network is proposed in [33]. In this paper the author proposes as an algorithm to obtain the location of the sensor node by using Time-of-Arrival (TOA) information along with four reference peer sensor node position information. This algorithm is based on the centroid algorithm. In paper [19], the author discusses the accuracy of indoor navigation system considering the Time-Difference-of-Arrival (TDoA) method for multipath components. In this method they employ Kalman filter technique to identify the multipath signals. Also, the receivers have the ability of movement in their experiments. The [10] is another paper which proposes a similar technique for wireless localization using Time-Difference-of-Arrival (TDoA) but it uses some sophisticated methods such as root multiple signal classification (MUSIC) and correlation techniques along with special COST-207 Channel model. The experiments in the paper were directed towards E-911 calls and locating the location of the origin of these calls but the authors concluded stating that they were unable to meet the FCC requirement accuracy for E-911 calls.

3.5 Navigation using Angle-of-Arrival (AoA)

In [49], we can find an indoor navigation system using Angle-of-Arrival (AoA) technique for 2.4 GHz radio signals. The paper performs the evaluation of the MVDR, Beamscan, root MUSIC and ESPRIT algorithms for Angle-of-Arrival (AoA) estimation with a simulator. In [6], we can find another indoor localization system for ad-hoc networks using Complex Angle-of-Arrival (AoA) technique. The paper proposes a better technique than conventional Angle-of-Arrival (AoA) technique and provides better results.

Chapter 4

PROBLEM STATEMENT

4.1 Problem Statement

In order to satisfy the requirements mentioned in Chapter 1, we face a number of research challenges, such as the definition of efficient node discovery and link set up protocols in the presence of heterogeneous and multi-interface devices, the design of suitable algorithms for performing opportunistic data exchanges and the related localization estimate, the analysis of the trade-offs between different performance indexes (energy consumption and protocol overhead as trade-offs for localization accuracy), not mentioning the reliability, confidentiality and security issues.

In this thesis, we address a more focused subset of the aforementioned problems. More specifically, we investigate the accuracy of range between the reference peers and the target node, estimated by the target node using the Euclidean and Statistical Time of Arrival (TOA) method. Although the Euclidean TOA method estimates the distance between a peer and the target node with a large error (about 20%) and Statistical TOA method estimates the distance with less error compared to Euclidean (about 10%), we can reduce the position error by using the following methods. We apply these preliminary results of approximate range analysis to a localization technique based on Linear Matrix Inequality (LMI) and Grid method. We further investigate improvements on the accuracy of localization by applying simple Barycentric algorithms or Center of Gravity(COG) along with the raw LMI and Grid method results obtained over time. Using a combination of these three methods and with multiple reference peer nodes, the error in position estimation can be reduced to less than a meter.

4.2 Conceptual Approach

In this thesis, we considered a system of mobile nodes equipped with a common communication device (e.g. Wi-Fi, Bluetooth or ZigBee). We consider a node, called Target, which is incapable of self-localization using any of the techniques such as Global Positioning System (GPS), Ultra wideband (UWB) or ultrasounds transceiver. Whereas other nodes, named reference peers, can perform self-localization with a certain accuracy which varies in time. The distance between the target node and other peer nodes is estimated using a technique known as Euclidean Time of Arrival (TOA) [56] or Statistical Time-of-Arrival (TOA). In this method, the target node broadcasts a short Hello message containing an accurate time and then the peers which receive this message respond with a packet containing its position information, position error and time. Using this information, the target node estimates its distance from each peer node, based on their time of arrival. The results of this method are utilized to form inequality equations [12] which are fed to a technique called Linear Matrix Inequality (LMI) to derive the the location of the target node. The general form of Linear Matrix Inequality is as shown in Equation 4.1

$$F(x) = F_0 + \sum_{i=1}^m x_i F_i > 0 \quad (4.1)$$

where $x \in R^m$ is the variable, $F_i \in R^{n \times n}$, $i = (0, 1, \dots, m)$

This standard form is transformed into 2x2 matrices using Schur Complements technique[58]. For every peer node, we obtain one 2x2 matrix. Thus the number of matrices obtained is equal to the number of peer nodes that are within the communication range of the target node. These matrices are further solved to obtain the position of the target node using a Software tool called MatLab as a proof of concept that this technique can generate accurate results. However, in the actual implementation of this technique, the target node will be equipped with the mathematical software to solve these matrices. Further, the location results are improved over time by employing a simple Barycentric algorithm or Center of Gravity (COG). The barycentric algorithm estimates the barycenter of two or more positions obtained from Linear matrix Inequality (LMI) or Grid

method whereas the Center-of-Gravity (COG) technique obtains the center of the cluster of positions calculated by Linear Matrix Inequality (LMI) or Grid method over time.

4.2.1 Assumptions and Goals

We begin with discussing the assumptions made to successfully develop the self-localization system. Firstly, the Target node along with all the in-range reference peer nodes are stationary during the the time of communication in order to exchange the necessary data for position estimation of Target node. Secondly, all the nodes are equipped with IEEE 802.11a/g/n radio for communication. Third, there is at least three in-range reference peer node to obtain the position of the target node with the accuracy.

Based on these assumptions, our goals are as follows. First, the Time-of-Arrival (TOA) technique has to obtain the Round-Trip Time (RTT) taking into account the radio signal interferences. Second, the Euclidean and Statistical Time-of-Arrival (TOA) techniques should utilize RTT collected from the kernel of the Target node and provide distance between reference peers and target node with acceptable accuracy. Third, the Linear Matrix Inequality (LMI) and Grid method should produce accurate position estimate using the data provided by the ranging technique along with the co-ordinates of the reference peer nodes. Fourth, the Barycentric Algorithm or Center-of-Gravity (COG) technique should improve the accuracy of position obtained from Linear Matrix inequality (LMI) and Grid method over time.

4.2.2 Time-of-Arrival Ranging Technique

There are many ranging technique to calculate the distance between two nodes such as Angle-of-Arrival (AOA) , Time-of-Arrival (TOA) , Time Difference of Arrival (TDOA), Received Signal Strength Indicator (RSSI) etc. We chose Time-Of-Arrival (TOA) technique compared to other as it is accurate, reliable, cost-effective and simple to implement. Time-of-Arrival is a distance based ranging technique which involves the exchange of messages between two or more nodes to collect

the Round-Trip-Time (RTT) in order to obtain the distance between the nodes. The Round-Trip-Time (RTT) is calculated at the driver IEEE 802.11g MAC layer of the FreeBSD/Linux kernel. Each device equipped with Self-localization capability is installed with FreeBSD/Linux kernel.

4.2.3 Linear Matrix Inequality Technique

Linear Matrix Inequality (LMI) is a mathematical solution to solve the optimization problems. In computer science and mathematics, an optimization problem is the problem of finding the best solution among all the feasible solutions. Among a large variety of optimization problems, we chose Linear Matrix Inequality (LMI) as it can easily be solved using the MatLab's Robust Control Toolbox software [25]. In order to find the position of the target node using the co-ordinates of reference peer nodes along with the respective distances obtained from the Euclidean or Statistical Time-of-Arrival (TOA) technique, we convert the raw data into 2x2 matrices. The number of 2x2 matrices is directly proportional to the number of in-range reference peer nodes. The general definition of Linear Matrix Inequality (LMI) mathematically is as shown in equation 4.1.

In our Linear Matrix Inequality (LMI) equations the constraints are non-linear in nature compared to linear constraints which can be solved using Linear Programming (LP) [28]. The possible position of the target node is an intersection area of all the reference peer node circles for unit-disk ranging model or reference node donuts for donut-disk ranging model. So, the constraints on the optimization problem is non-linear.

4.2.4 Grid Method

Grid method is a technique designed by us to obtain the position of the target node using the reference peer node co-ordinates and the distances between each reference peer node and the target node obtained from the Euclidean or Statistical Time-of-Arrival (TOA) technique. In this method we use a technique called multilateration in which we obtain the intersection area of all the circles or circle donuts formed using the co-ordinates of the reference peer node as the center of each circle or circle donut with the Time-of-Arrival (TOA) distances as the radius respectively

obtained from Euclidean or Statistical TOA techniques. These circles or circle donuts are formed on a surface which is formed by 1m-by-1m grid points. After laying all the circles or circle donuts on this grid we obtain all the grid points contained inside the intersection area of all these circles or circle donuts. The reason we obtain grid points only from the intersection area is because the intersection area has the highest probability of containing the target node position. So, after we obtained all the grid points from the intersection area of all the circles or circle donuts we perform the Center-of-Gravity (COG) technique to obtain the center of this cluster of grid points which is the estimated position of the target node calculated by Grid method.

4.2.5 Barycentric Algorithm

Barycenter is defined as the center of mass of two or more bodies and barycentric algorithm uses this definition and applies to position co-ordinates of the target node. The accuracy of the estimated position co-ordinate of target node obtained from Linear matrix Inequality or Grid method can be improved over time by collecting more position co-ordinates i.e., the target node can wait a little longer in the same position to collect more Time-of-Arrival (TOA) data from new reference peer nodes which were not in-range for the first try of communication but are available in successive tries. After obtaining more than one position for the target node we can use the barycentric algorithm to calculate the barycenter of all the estimated target node positions which will provide better accuracy than raw Linear Matrix Inequality (LMI) results. As the positions of target nodes do not have any mass, it is assumed to be unit mass during calculation of barycenter using the barycentric algorithm.

4.2.6 Center-of-Gravity Technique

Center-of-Gravity (COG) is a geometric property of an object and is defined as the average location of the weight of an object.

Chapter 5

DESIGN AND METHODS

5.1 Ranging Model

The ranging model is considered to have a simple unit-disk model for Radio propagation with a range R within which it can communicate with all the in-range peers opportunistically. We assume that the radio signals are not received outside the distance R from the transmitter. Although the above assumptions are made to simplify our simulation, the results are also applicable to more general non-unit disk models. Every node in the network is equipped with a common wireless communication interface (e.g. Wi-Fi, Bluetooth or ZigBee) that is used for opportunistic data exchanges. The target node periodically communicates with peer nodes for a period of time called the Scan Phase which is repeated with period T . The ratio between the scan phase and the entire cycle time, T , is called duty cycle and is denoted by δ . Only the target node uses this scan period T ; peer nodes respond to the target node through request-response communication. During the scan phase, the target node estimates its position and ranging by executing the following algorithms: Euclidean TOA or Statistical TOA, Linear Matrix Inequality or Grid Method and Barycentric algorithms or Center-of-Gravity (COG).

At the beginning of the scan phase, the target node broadcasts Positioning Inquiry (PI) messages to peer nodes within range. This will be integrated with the OLSR (Optimized Link State Routing) Hello messages with modifications to the request-response protocol [27]. Peer nodes will respond with their position estimates, estimation error, and Unique Identification (UID).

The target node then computes imprecise range estimate with each peer node using the Euclidean TOA or Statistical TOA ranging method. The imprecise range estimate gives a range accuracy of only about 15 meters (20%) for Euclidean TOA whereas the Statistical TOA provides an accuracy of about 10 meters (13%), but the range accuracy will be improved to about 1 to 3

meters (2%-3%) for a range of 200 meters in the next stage when they are used as inputs to the LMI or Grid Method and barycentric algorithm/COG technique. Through the LMI/Grid method and COG technique, more accurate range estimates will be computed as compared to the LMI and barycentric algorithms.

5.2 Ranging techniques

In this section we will discuss the 2 ranging techniques we utilize in computing the distance between the Target node and the reference nodes. There are many ranging techniques apart from Euclidean Time of arrival and Statistical Time of Arrival such as Angle of Arrival, Received Signal Strength Indicator (RSSI), Time Difference of Arrival (TDOA) etc. [3].

5.2.1 Euclidean Time-of-Arrival Ranging Method

In the Euclidean TOA ranging method, a large number of Round Trip Time (RTT) between two wireless nodes are measured [56]. Then we compute the Euclidean Distance (ED) between this set of RTT and known sets of RTT for different distances (for the same Wi-Fi communication devices). The Round Trip time (RTT) is very widely used in ranging techniques to compute the Time of Arrival (TOA) of a packet sent from the Station (STA) to an access point (AP). In our technology we call station as the Target node and the Access Point is called Reference Node.

The RTT can be measured in IEEE 802.11g using data and acknowledgement (ACK) messages at the driver layer, in which timestamps (in nano-second) are collected when data are sent and ACK messages are received. The time differences between those two events (or interrupts) are considered the RTT for delivering these packets. The target node will send the data while the peer nodes will respond with the ACK messages, whereby the RTT can be computed at the target nodes.

Our current results show that with the help of ED, we only need less than 40k samples to achieve ranging accuracies of 3 meters and 15 meters for indoor and outdoor scenarios, respectively. Even though the accuracy of this imprecise range estimate is still low, the accuracy of

the target node position will be improved using the Linear Matrix Inequality/Grid method and Barycentric Algorithm/Center-of-gravity technique.

5.2.2 Statistical Time-of-Arrival Ranging Method

The Statistical Time-of-Arrival ranging method has two stages: first is to collect the round trip times for the packets, and second is to match the probability density estimate of the collected samples against the density estimate of the stored reference databases for different distances to determine the target node distance from the reference nodes. We could employ the Euclidean distance measure to compare the timings of the real time data and the stored reference data timings, but due to the nature of the wireless propagation and the noise in Round-Trip-Time (RTT) measurements, this is error prone. Ideally we would use this Round Trip Time (RTT) and compute the distance using the distance, time and speed equation, but the RTT collected through the driver layer of the device consists a lot of noise and is prone to produce a huge error in the position of the Target node. In our method, we construct a probability density estimate and use statistical distance measures such as the Bhattacharyya Coefficient and Kullback-Liebler divergence to determine the distance between the target and the reference nodes. We propose to use the Bhattacharyya Coefficient as it is very simple, robust and is symmetric.

The Bhattacharyya coefficient measures the relative closeness of the probability density functions of the two random variables. In the continuous case, it measures the similarity of density functions, while in the discrete case, it measures the similarity between the probability mass functions.

Let us consider two random variables, A and B. Their probability density functions are given as $f_A(x)$ and $f_B(x)$. Then the Bhattacharyya coefficient is given by,

$$BC(A, B) = \int \sqrt{f_A(x)f_B(x)}dx \quad (5.1)$$

In the discrete case, let $p(x)$ and $q(x)$ be the probability mass functions of A and B.

$$BC(p, q) = \sum_x \sqrt{p(x)q(x)} \quad (5.2)$$

The Bhattacharyya distance is then given by,

$$D_B(p, q) = -\ln BC(p, q) \quad (5.3)$$

In either case, $0 \leq BC(p, q) \leq 1$ and $0 \leq D_B(p, q) \leq \infty$. It is important to note that the $D_B(p, q)$ does not satisfy the triangle inequality condition and hence does not form a metric.

In each experiment, we considered two nodes, the target and the reference. The target node initiates the communication with the reference and after the initial handshaking, the traffic is sent out. The time taken for each packet to reach the reference node, plus the time taken for the ACK (to the sent packet) to reach the target is the Round Trip Time (RTT). This is measured repeatedly so as to collect the round trip times for 65536 (216) packets. The RTT data is collected for different distances 10, 20, 30m. Figure 5.1 shows the histograms for 10m. Also shown is the probability density function (PDF) of the histograms. This is an estimate of the probability density function (PDF) obtained from the ksdensity function of MATLAB.

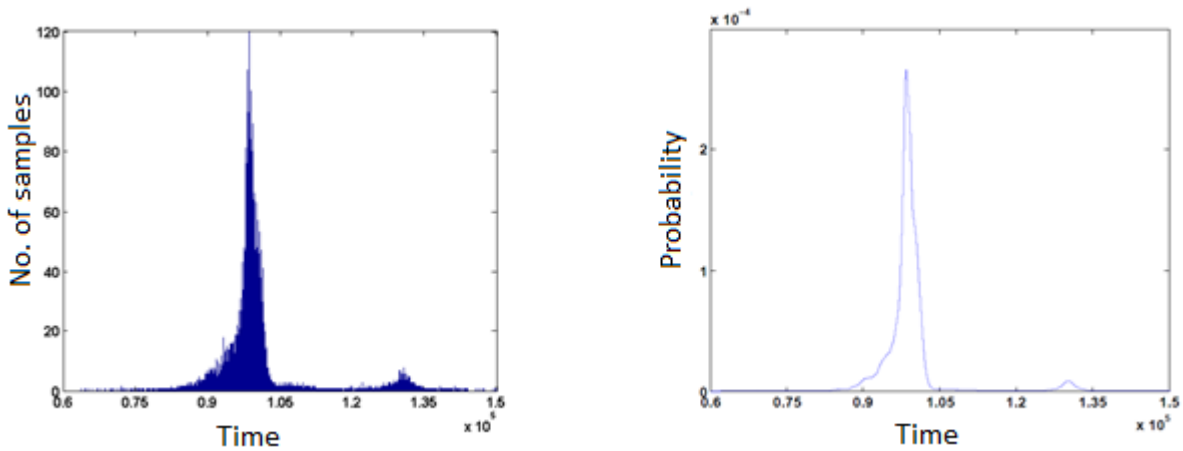


Figure 5.1: (a) Histogram of RTT samples for reference node at 10m and (b) Probability density estimate of RTT samples for reference node at 10m

Similarly, we can see the probability density functions for reference node at 20m and 30m in Figure 5.2 and Figure 5.3 respectively.

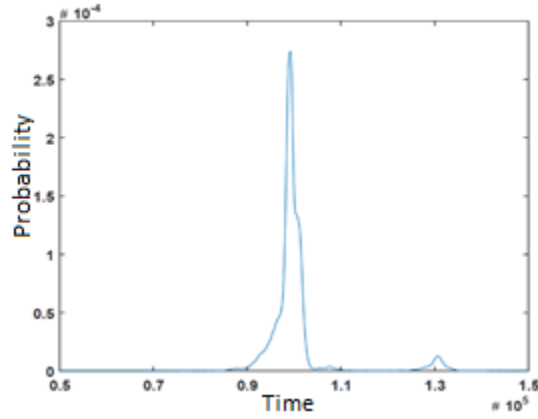


Figure 5.2: Probability density estimate of RTT samples for reference node at 20m

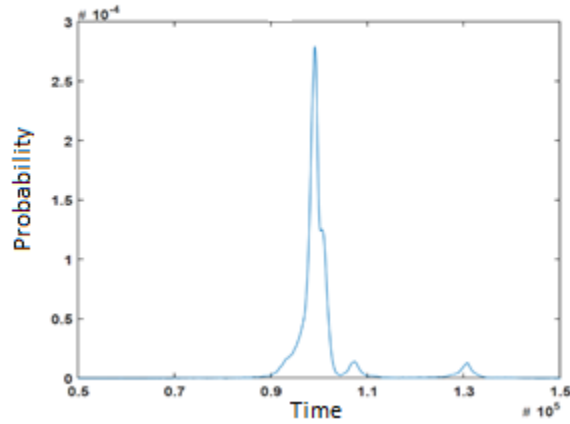


Figure 5.3: Probability density estimate of RTT samples for reference node at 30m

5.3 Self-Localization of Target Node

In this section we consider the self-localization of target node based on position information and imprecise ranging data from peer reference nodes. When a target node is estimating its position, it stays at a fixed position for a given time interval W during the Scan Phase period while

it broadcasts PI messages to its peer nodes, receives position estimates along with estimation error from peer nodes, computes imprecise ranges to the peers using Euclidean/Statistical Time of Arrival ranging technique, and finally estimates the position of the target node using the Linear Matrix inequality/ Grid method, barycentric algorithms and Center-Of-Gravity technique.

Each peer node has its own self-localization capabilities. We denote by P_i and P'_i the real and self-estimated position of peer # i . We assume the estimation error $e_i = |P_i - P'_i|$ can be modeled as the module of a two-dimensional Gaussian Random Variable $[x(t), y(t)]$, with zero mean and variance of σ^2 .

The position estimation time t is measured in number of scan periods, starting with time $t = 1$. During each position estimation time, the method consists of two stages: first is the Raw Linear Matrix Inequality/Grid method estimation and the second being the Barycentric algorithm and Center-of-gravity technique. Each of these techniques are explained in details in the following subsections.

5.3.1 Raw LMI Estimation

At every scan period t , the target node collects self-localizing estimates from each peer node that is within range when they respond to its PI broadcast message. Let $em_i = \max_t(e_i(t))$ denote an upper bound on the error between the real and estimated position of Peer i , such that

$$|P'_i(t) - P_i(t)| \leq em_i \quad \text{for} \quad t \geq 1 \quad (5.4)$$

Let $P_T(t)$ be the real position of the target node. Let the maximum error in the imprecise range estimation using Euclidean/Statistical TOA ranging be er_i . Also, let the imprecise range between the target and a peer node as computed to be R' . Then we have

$$(R' - er_i) \leq |P_T(t) - P_i(t)| \leq (R' + er_i) \quad (5.5)$$

Hence, for each Peer # i within the range of the target node at time t , inequality Equations 5.4 and 5.5 yield the triangular inequality Equation 5.6.

$$(R' - er_i - em_i) \leq |P_T(t) - P'_i(t)| \leq (R' + er_i + em_i) \quad (5.6)$$

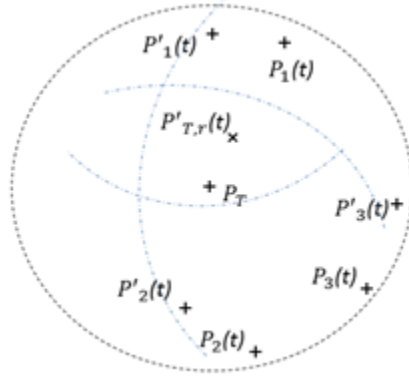


Figure 5.4: Raw Position Estimation using only Linear Matrix Inequality

A set of Equation 5.6, collected for all the peers in the coverage range of the target node, form a Linear Matrix Inequality (LMI) that can be solved using standard techniques. The resulting solution is used as a raw LMI estimation $P'_{T,r}(t)$ of the target position. The solutions that satisfy the mathematical constraints defined in the LMI will improve the accuracy of the position and range estimates from the original imprecise range estimate computed from the Euclidean/Statistical TOA ranging technique. Figure 5.4 shows how $P'_{T,r}(t)$ is generated at cycle t , assuming that only P_1, P_2 and P_3 are within the target node range at time t .

5.3.2 Self-Localization using Linear Matrix Inequality and Barycentric Algorithm

Using all the raw LMI estimations computed since $t = 1$, the barycenter of these estimations is defined as the self-localizing estimation of the target node at time t , i.e.

$$P'_T(t) = \frac{\sum_{k=1}^t w_k P'_{T,r}(t)}{\sum_{k=1}^t w_k}, \quad t \geq 1 \quad (5.7)$$

The variable w_k is the weighing coefficient which is proportional to the number of peers that have contributed to the k^{th} LMI estimates. We consider $w_k = 1$ for best results [59] .

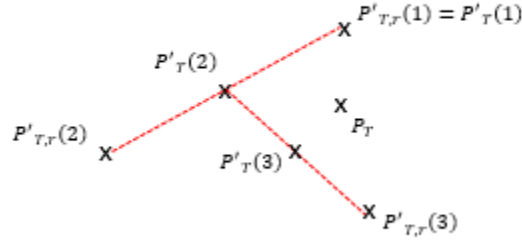


Figure 5.5: Position Estimation using Linear Matrix Inequality and Barycentric Algorithm

Figure 5.5 illustrates the second stage after the raw LMI estimation where a more accurate position estimate is generated over the time $t > 1$. It shows how $P'_T(1), P'_T(2)$ and $P'_T(3)$ are generated from $P'_{T,r}(t)$, at $t = 1, 2, 3$ with all weights w_k equal to 1.

The above self-localizing estimates will improve over time and with more number of in-range peer reference nodes.

5.3.3 Self-localization using Linear Matrix Inequality and Center of Gravity Technique

The center of gravity (COG) technique is equivalent to centroid of a cluster of points whose masses are considered to be unit mass. The center of gravity and center of mass for any arbitrary body are the same. In our technology we have used the COG technique to calculate the center of a cluster of Target node positions which are generated after every iteration. Using all the raw LMI results tabulated over N iterations is then used to calculate the Center of Gravity (COG) by using the Equation 5.8.

$$C = \frac{\sum_{i=1}^N P_i}{N} \quad (5.8)$$

In Equation 5.8, C represents the Center of gravity of the cluster of estimated target node positions, N is the total number of iterations/Grid Points and P_i is the target node position coordinate of the i^{th} iteration.

5.3.4 Self-positioning using Grid Method Technique

Grid method is based on the multi-lateration technique of finding the exact location of target node when there are more than three reference nodes. In this method we generate intersection area of all the reference nodes with center being the reference node positions and radius being the TOA distance estimated by the target node from the reference nodes using either Euclidean or Statistical TOA technique. We map out the entire intersection area with small 1m x 1m grids in order to generate a cluster of points inside the intersection area. These cluster of points is then utilized using the Center-of Gravity (COG) method to generate a single point which is the Target node estimation generated from Grid method. The assumption made during this technique is that the target node is present inside the intersection area of all the reference nodes. The MatLab figure of the Grid method with grid points and reference nodes with multi-lateration is as shown in the Figure 5.6.

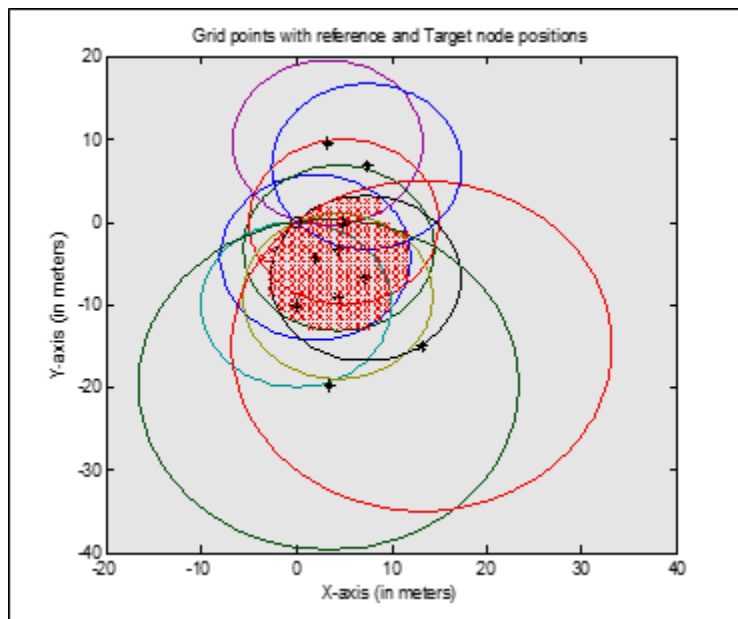


Figure 5.6: Plot of all the grid points in the intersection area including the reference node and real target node positions

Chapter 6

IMPLEMENTATION

6.1 Simulation Setup and Implementation

The models described in the previous section have been implemented using MatLab R2013a and its Robust Control Toolbox which provides an LMI solver. In this section, we define a reference test case and study the impact of the selected parameters on the accuracy of the calculated range and the accuracy of position (time dependent).

6.2 Reference Case

Table 6.1: Reference case parameters

Parameter	Value
N	10-200
T	1s
σ_i	100%
ρ	0
w_T	0s
R	100 meters
δ	50%
Area	200m x 200m
W	120s
α	20%

6.2.1 Linear Matrix Inequality with Barycentric Algorithm

Our reference case involves $N = 10$ to 200 peer nodes moving in a 200m x 200m square and one target node remaining at the center of the square. Target node and peers share the same radio range $R = 100$ meters, so that all of the peers that are within range of the target node at each time are considered for position estimation. Peers and target node also have the same scan period T

= 1 second and the same duty cycle $\delta = 50\%$, so that duty cycles are always partially overlapped [59]. The scan period of the target node starts at $t = 0$ while the scan period of each peer starts with an offset which is uniformly distributed in $(0, T)$. In the reference case, the accuracy of each peer position obtained by some non-opportunistic technique has been set to $\sigma_i = 100\%$ and it is assumed to be constant over time. Furthermore, the self-positioning estimates are not correlated, i.e. $\rho = 0$ and the accuracy of the range calculated using Euclidean TOA has been set to $\alpha = 20\%$, which is also assumed constant over time.

The target node, placed in the center of the area, estimates its position using the opportunistic localization model defined in Section 5.3. The opportunistic localization time for the target node is set to $W = 2$ minutes and the warm-up time is set to $w_T = 0$ second for best results [59]. The performance of the target node's opportunistic positioning scheme is evaluated in terms of distance between real and estimated position $|P_T - P'_T(t)|$. Table 6.1 summarizes the parameter values used for the reference case.

6.2.2 Linear Matrix Inequality with Center Of Gravity Technique

The simulation setup for the Linear Matrix Inequality (LMI) and Center-of- Gravity (COG) technique remains similar to the setup of Linear Matrix Inequality (LMI) and Barycentric algorithm as given in Section 6.2.1. But the difference remains that after the raw LMI results are collected over time, we apply Center-of-Gravity (COG) technique as shown in Section 5.3.3 instead of Barycentric algorithm. In this method we considered $N = 5$ to 50 peer nodes with three different communication range which are 20m, 30m and 40m. The Target node also follows the same communication range as the peer nodes respectively.

6.2.3 Varying Time-of-Arrival Induced Error

This section is setup in exactly the same manner as Section 6.2.2. The Time-of-Arrival(TOA) induced error is the error in the distance estimation measured by the Euclidean or Statistical Time-of-Arrival (TOA) ranging technique between the peer nodes and the Target node. We vary the

Time-of-Arrival induced error from 10% to 50% and evaluate the estimated Target node position error obtained using the Linear Matrix Inequality (LMI) and Center-of-Gravity (COG) technique. We also vary the number of peer nodes from $N = 5$ to 30 peer nodes to test the accuracy of the Target node Position.

6.2.4 Random Waypoint Mobility Model Analysis

In Ad Hoc networks the mobility of the nodes is an important aspect and is a challenge to simulate the real world mobility of nodes. There are many mobility models proposed but in this thesis we choose Random Waypoint mobility model (RWMM) for its simplicity and wide acceptance by researchers. In random-based mobility models, the mobile nodes move randomly and freely without restrictions. To be more specific, the destination, speed and direction are all chosen randomly and independently for each node.[7]

In simulation, each mobile node randomly selects one location in the simulation field as its destination. It then travels towards this destination with constant velocity chosen uniformly and randomly from $[V_{min}, V_{max}]$, where the parameter V_{min} is the minimum allowable velocity for every mobile node and V_{max} is the maximum allowable velocity for every mobile node. The velocity and direction of a node are chosen independently of other nodes. Upon reaching the destination, the node stops for a duration defined by the pause time parameter T_{pause} . If $T_{pause} = 0$ then it is a continuous mobility model with no pause. After T_{pause} duration, the node chooses another random destination in the simulation field and the process runs until the simulation end time has been reached. The reference peer node positions are obtained at every instance of time $t = 1$ sec and this process is carried out until the simulation end time. Therefore the simulation end time is the same as the total number of reference peer node position of all the in-range reference peer nodes.

6.2.5 Firefighter Mobility Model Analysis

The firefighter mobility model is modified mobility model targeted to simulate a real firefighter movement inside a fire scene (Building). The model has been developed by taking in the input from the interviews with many fire departments including Auburn Fire department, New York Fire department, Atlanta fire department etc. Part of Firefighter mobility model MATLAB code is similar to Random Waypoint Mobility model but the design of the simulation model is entirely different. The fire building is usually divided into four zones, which may be named as Zone A, B, C and D respectively. During a fire event, the Fire Chief in charge of the event allocates a respective zone to a group of firefighters in order to distribute all the firefighters around the building. The Chief also assigns a specific task to the group. The firefighters use the Hoes line to enter and exit the building and do not lose contact with the hoes. If the firefighters have to leave the hoes line in order to check a particular room then they will hook a fire resistant rope to the hoes line in order to prevent themselves from getting lost inside the building. Our simulation model follows the above strategy to simulate the firefighter movement in their respective zones.

In order to simulate a real world fire event with firefighters working in their respective zones assigned by the Fire Chief-in-Charge of the scene, we restricted the movement of firefighters outside their zones. This means that the firefighters are free to move anywhere inside their zone but will not be able to move outside of their zone and will not be able to migrate from one zone to another during the simulation time. We randomly assign a group of firefighters to each zones of operation depending on the number of firefighters on the scene. For example, if we have 20 firefighters on the scene then there will be five firefighters in each zone. The movement of firefighters inside their zone is randomly chosen similar to Random Waypoint mobility model. The number of firefighter vary from $N = 5$ to 30 and the simulation time is chosen to be $t = 500$ sec. The position of the each firefighter is tabulated into separate arrays with X- coordinate and Y-coordinate respectively. This tabulation is done every 2 sec, which means that we have 250 different positions of each firefighter. We use the first 200 positions of each firefighter to calculate the lost firefighter position (Target Node) using Linear Matrix Inequality (LMI) and Grid Method. After generating

200 target node positions, we use the Center-of-Gravity (COG) to calculate the final target node position.

Table 6.2: Firefighter Mobility Model parameters

Parameter	Value
N	5-30
Walk Interval	1-1.5m/s
Pause Interval	0-6s
Simulation Time(t)	500s
R	30 meters

6.3 Real-World Model Specifications

After testing our technology with simulation models we designed a real-world device to test our technology with real-world data. The important specification for the real-world device is given in Table 6.3.

Table 6.3: Real-World Model Specification

Specification	Value
Network Card	Ubiquiti Networks SR-71 (mini-PCIe)
Processor	Intel Atom D510 and N270
CPU Frequency	1.6 GHz
Communication Frequency	2.4 GHz
Data Rate	24 Mbps
Wireless Protocol	IEEE 802.11 b/g
OS Kernel	FreeBSD/Linux

Chapter 7

PERFORMANCE EVALUATION

7.1 Simulation Result

In this chapter we will discuss all the results obtained from the simulation setup of Chapter 6. After discussing all the simulation results we will also discuss details of the real-world experiment results obtained by performing the results from a real setup indoor and outdoor.

7.2 Accuracy of reference case

This section of the chapter discusses the results obtained from the reference case setup of Section 6.2.

7.2.1 Linear matrix Inequality with Barycentric Algorithm

The reference case for raw Linear Matrix Inequality (LMI) estimation method was run 30 times with different random seeds. The error estimation E of each run is tabulated as percentage error in the self-localization position of the target node throughout this chapter. The results show that the localization error of the target node is reduced as the number of peer nodes is increased, as illustrated by Figure 7.1.

The accuracy increases as the the number of peer nodes increases. The Barycentric Algorithm improves the accuracy of the model over time, so we considered $t = 5$ seconds in our reference model as an appropriate amount of time to get sufficient accuracy. The reference case for LMI+Barycentric algorithm estimation method has been run with different random seeds and the average localization error is as shown in Figure 7.2.

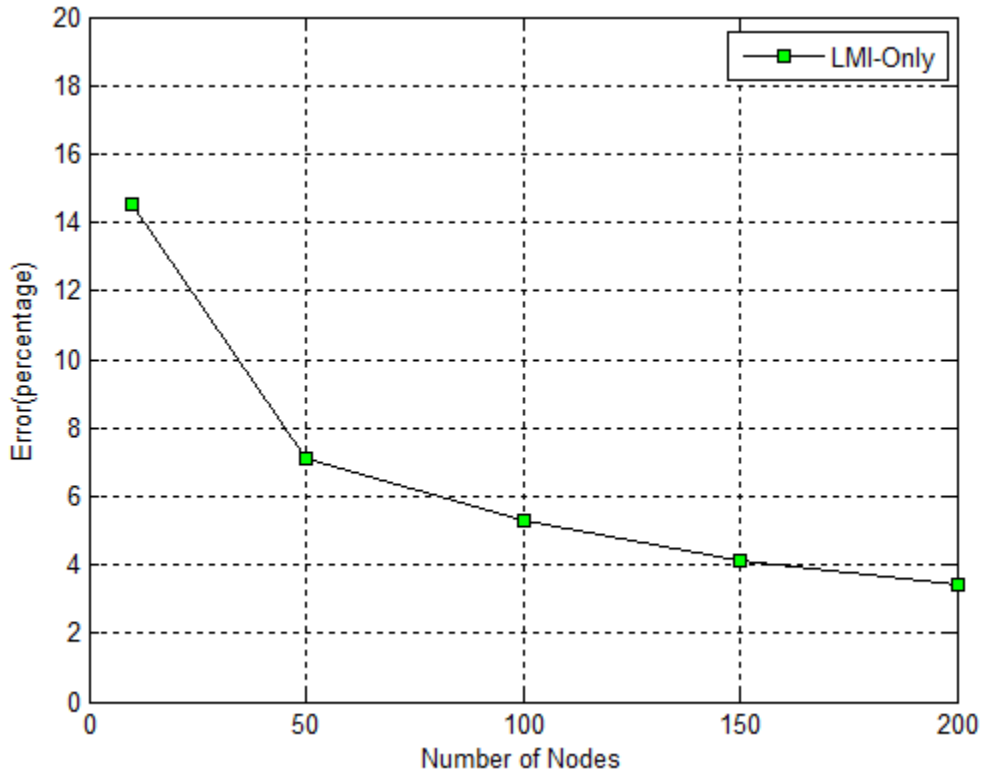


Figure 7.1: LMI-only Error Estimation

In this method, the percentage error has not been averaged over 30 runs as done with the raw LMI-Only method instead it is the percentage error of just a single run. The reader can easily visualize in the figures that the LMI with Barycentric Algorithm is better than raw LMI-only estimation and requires much less amount of time to achieve it.

To better understand the behavior of this model, we show in Figure 7.3 the error comparison of both LMI-Only as well as the LMI+Barycentric algorithm estimate. The percentage error in self-localization of the target node has been produced for 10 runs with a constant number of peer nodes ($N = 100$) within the 200m x 200m square area for both the techniques. The percentage error in both the cases have not been averaged and are just the result of a single run. From the figure, it is clear that the LMI+Barycenter method's accuracy increase with time and is better than the LMI-Only technique. The accuracy of the localization depends on the distribution of the peer nodes, which is random. These wide variations are likely to be ascribed to the different trajectories of

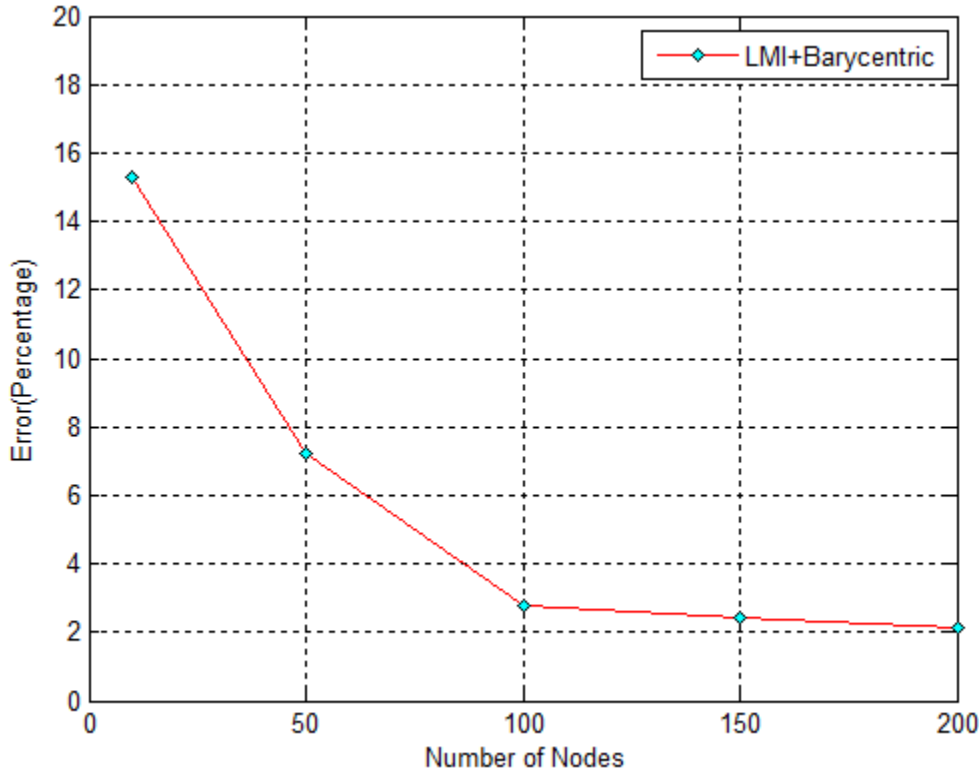


Figure 7.2: LMI+barycenter Error Estimation

peers in different runs. In fact, depending on the random seed of the run, if peers are widely spread out in space, then this leads to good LMI-only localization and, in turn, good LMI+barycentric algorithm estimation. On the other hand, if they are unevenly distributed in the area forming a small number of groups, then this will lead to poor LMI-only localization and, consequently, to a degradation of LMI+barycentric algorithm performance.

To further explain the variation of the position accuracy, we studied the cases by increasing the range of the target node from 100 meters to 150 meters and then to 200 meters while the rest of the parameters remain the same as the reference case in Section 6.2. Figure 7.4 depicts the MatLab plot of self-localization error (in percentage) of the target node utilizing raw Linear Matrix Inequality technique while Figure 7.5 depicts the MatLab plot of self-localization error utilizing both Linear Matrix Inequality as well as Barycentric algorithm.

The reader can clearly see from both the figures that the localization error remains *relatively* the same for all the considered range. This simulation result encourages increasing the range of

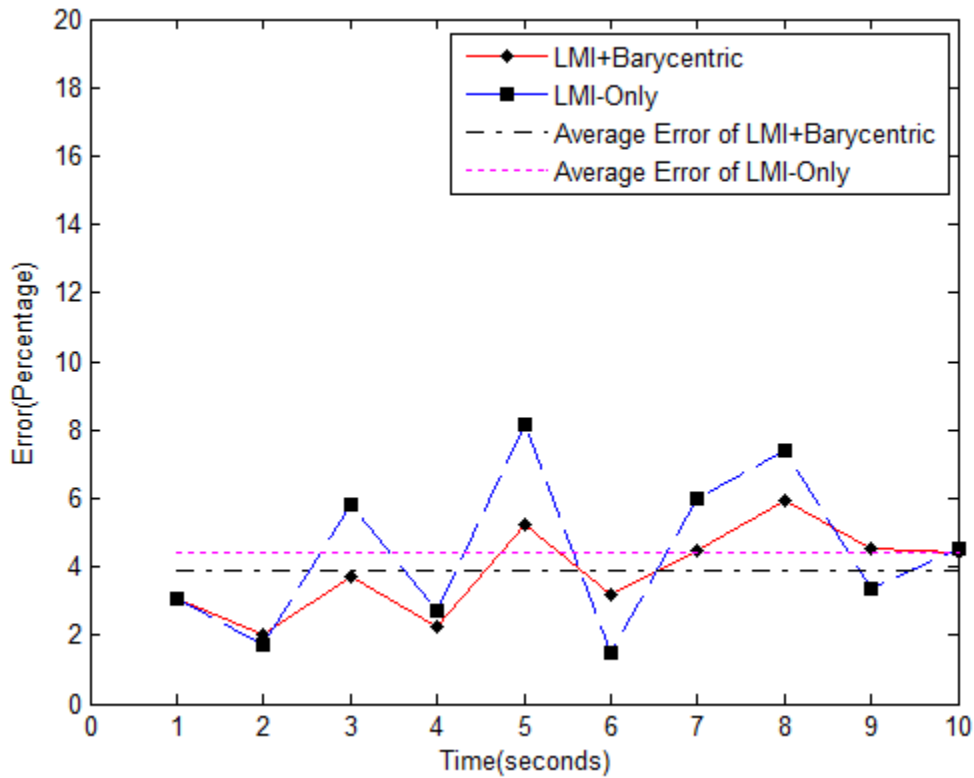


Figure 7.3: Error comparison Between LMI-only and LMI+barycenter

communication without suffering much error in the position of the target node which is a phenomenal achievement.

In most runs, the accuracy of the barycentric algorithm estimation tends to improve over time, where each additional raw LMI estimation contributes to improving the estimation, since new information is added.

In order to obtain the results for actual real world devices in which the range of the device is about $R = 20\text{m}$ located in a wireless environment (e.g. Wi-Fi) of $100\text{m} \times 100\text{m}$ square area. The range R of the device is considered to be a circular area of radius 20m . Thus, during any particular time only certain number of nodes within the square area are considered for self-localization as they are the only in-range reference peer nodes. In simulation we assumed that the total number of nodes in the $100\text{m} \times 100\text{m}$ area is $N = 200$ and the method implemented is LMI+barycentric

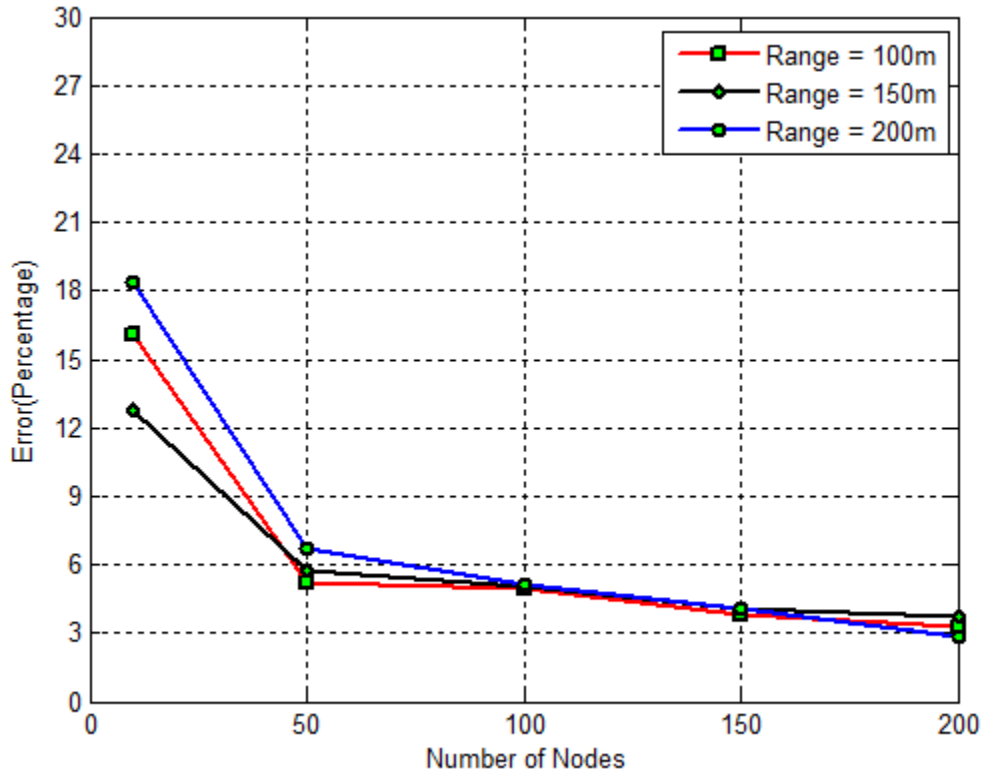


Figure 7.4: LMI-Only Estimation Error for Varying Node Range

algorithm technique for self-localization. Other parameters in this simulation are considered to be the same as in Section 6.2.

Figure 7.6 illustrates the percentage error in self-localization of the target node over 30 runs. The reader can clearly see that the average percentage error in the opportunistic self-localization is $E = 1.52\%$ (0.31m), which is very low compared to the error obtained from Euclidean Time-of-Arrival technique of 20%.

7.2.2 Linear Matrix Inequality with Center Of Gravity Technique

In order to understand the behavior of this model, we designed a simulation setup which has up to 50 peer nodes in-range to the Target node. Figure 7.7 is a MatLab plot which shows the variation of Position error in Target node position as the number of in-range peer nodes increases.

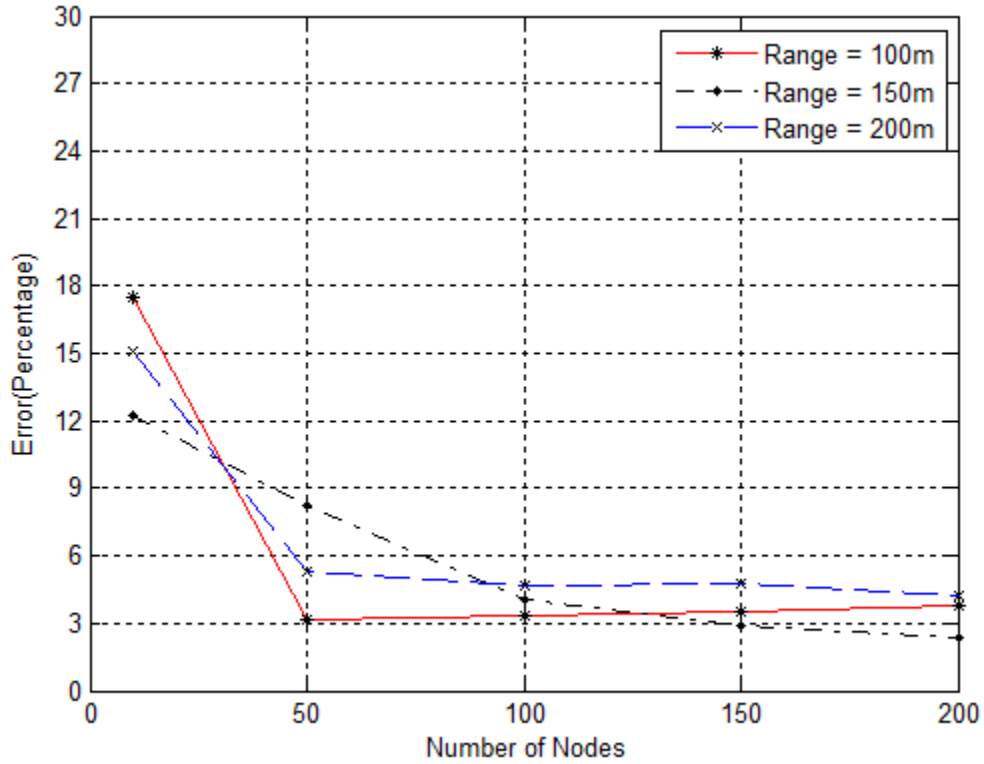


Figure 7.5: LMI+Barycenter Estimation Error for Varying Node Range

Figure 7.7 is a MatLab plot which depicts the positioning error (in percentage) of the Target node which is averaged after 50 iterations for better results. The curve for the communication range = 40m also indicates the 95% confidence interval in order to look at the accuracy of the results. It is clear from Figure 7.7 that the confidence in the result is very high which indicates that Center-Of- Gravity (COG) technique is better compared to Barycentric Algorithm. The Center-of-Gravity (COG) technique improves the accuracy of the Target node position calculated using Linear Matrix Inequality (LMI).

7.2.3 LMI with varying Euclidean Time-Of-Arrival Distance Error

Figure 7.8 shows a plot of varying TOA Error vs Number of nodes. The TOA error is the error in the distances between target node and Peer nodes obtained after the Euclidean TOA ranging method is performed. The error in this figure indicates the error obtained after the Target node

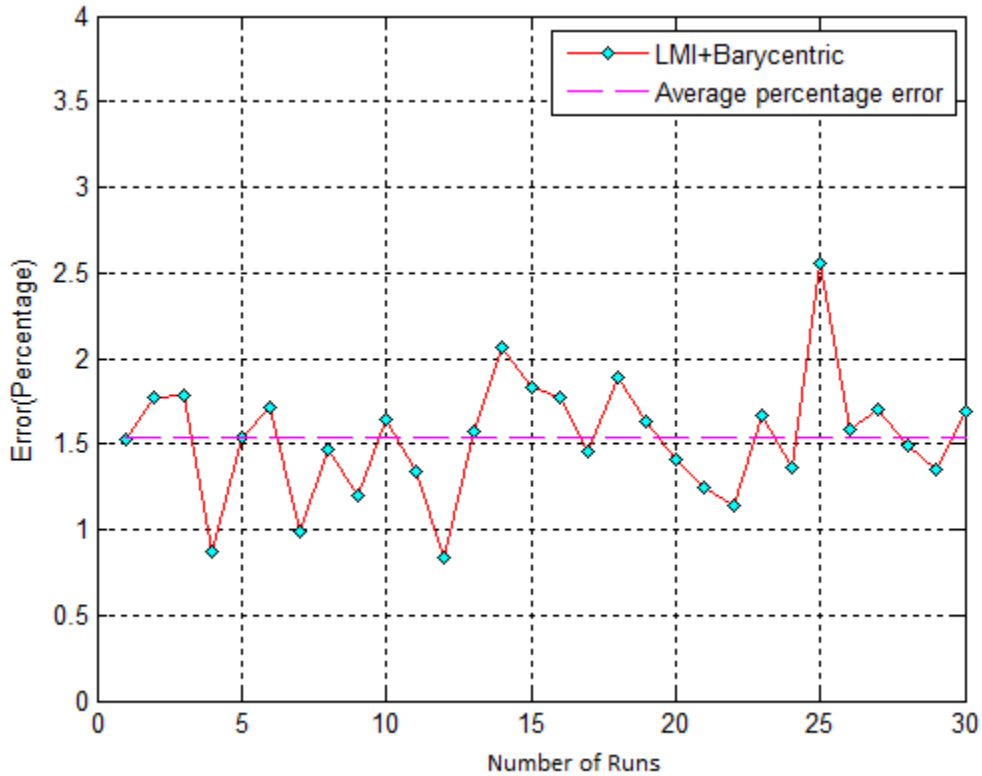


Figure 7.6: LMI+Barycenter Estimation for actual devices

position is calculated using LMI and COG techniques. It can be clearly seen from this figure that even though the TOA error is 50%, the Position error does not exceed 12%. This is a tremendous reduction in error by the LMI and COG techniques. Also, if the TOA error is as low as 10%, the Position error can be as low as 1%, indicating that the position obtained from our technique is very close to the real position of the target node.

7.3 Simulation Results of Mobility Models

In Section 7.2 we discussed the simulation results of the reference case setup of Section 6.2. During all those simulation cases the reference peer nodes along with target node did not have the capability of motion i.e., all the nodes were stationary during the Self-Localization of target node. But motion is an important aspect of Self-localizing nodes. In order to test our techniques for mobile nodes we designed a setup using mobility models as described in Section 6.2. In this

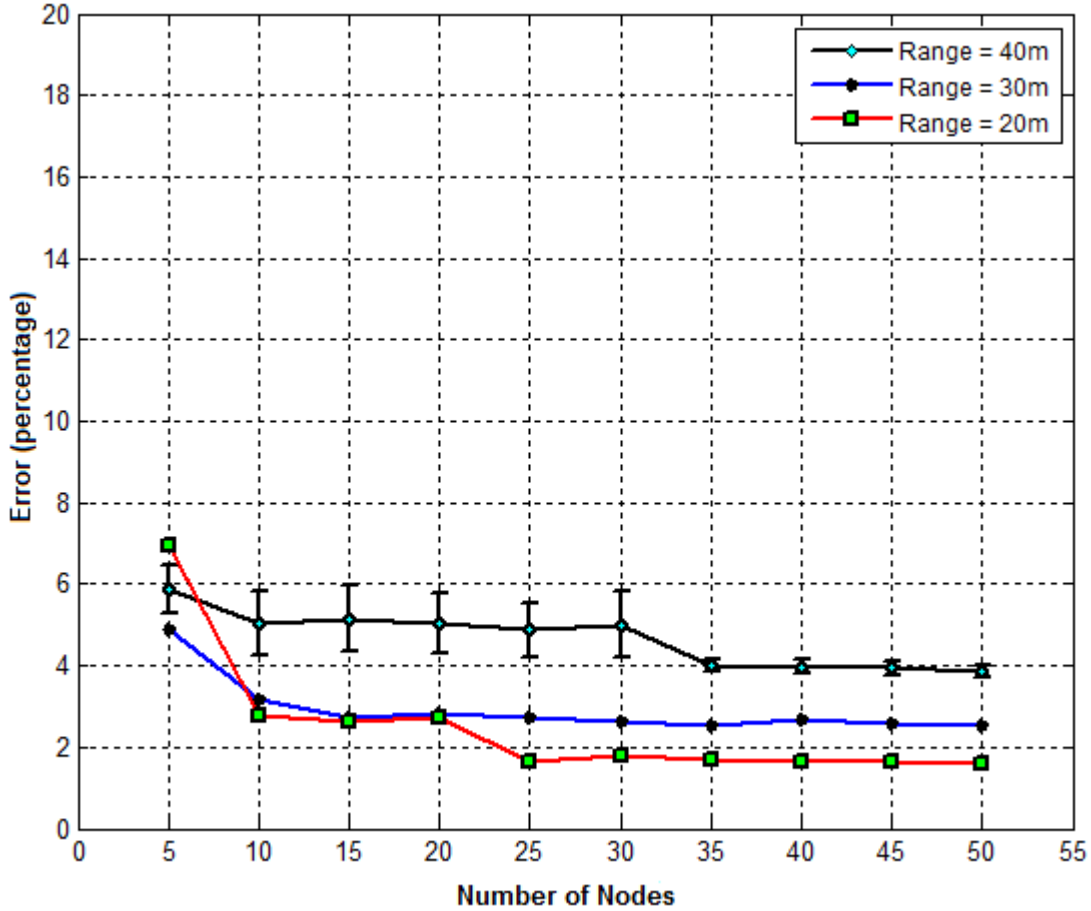


Figure 7.7: LMI+Center Of Gravity Estimation

section we will discuss the results obtained from the experiments conducted on the simulation setup of Section 6.2.

7.3.1 Linear Matrix Inequality with Random Waypoint Mobility Model

In the Random Waypoint model, V_{max} and T_{pause} are the two key parameters that determine the mobility behavior of nodes. If the V_{max} is small and the pause time T_{pause} is long, the topology of Ad Hoc network becomes relatively stable. On the other hand, if the node moves fast (i.e., V_{max} is large) and the pause time T_{pause} is small, the topology is expected to be highly dynamic. To prove this we have generated the simulation model with varying Pause times T_{pause} and a constant $V_{max} = 1.5$ m/s, the plot is as shown in Figure 7.9

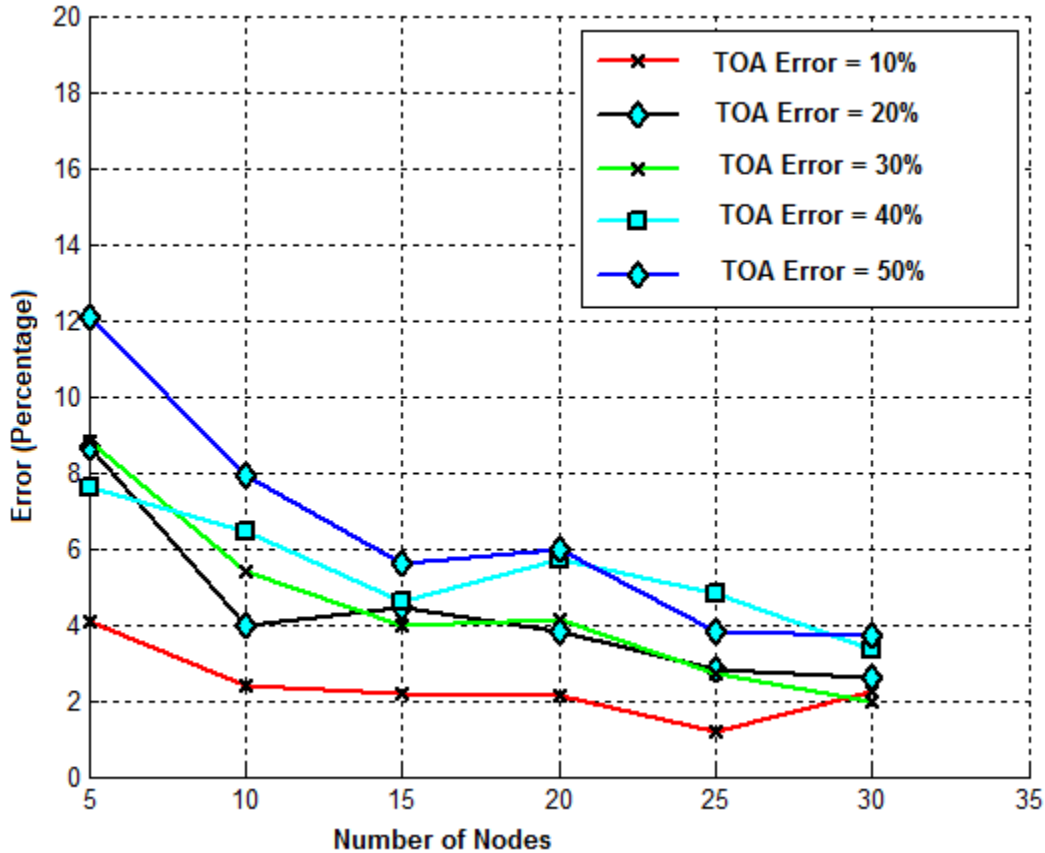


Figure 7.8: LMI+COG with Varying TOA error

Figure 7.9 shows that the Plot with Pause time $T_{pause} = 50\text{sec}$ is more stable compared to Pause time $T_{pause} = 0\text{sec}$, 10sec and 20sec . We can also notice that as the pause time increases the plot becomes more stable.

7.3.2 Linear Matrix Inequality with Firefighter Mobility Model

Figure 7.10 shows the plot of Error in the Target node position (in meters) versus the number of peer nodes (firefighters). From the plot it can be clearly seen that the accuracy of the target node position increases as the number of firefighters increase on the fire scene. The accuracy is 90.88% for just 10 firefighters on the scene, which is an excellent result. Also, the accuracy increases to 96.5% when the firefighter count increases to 15. In this plot the target node position does

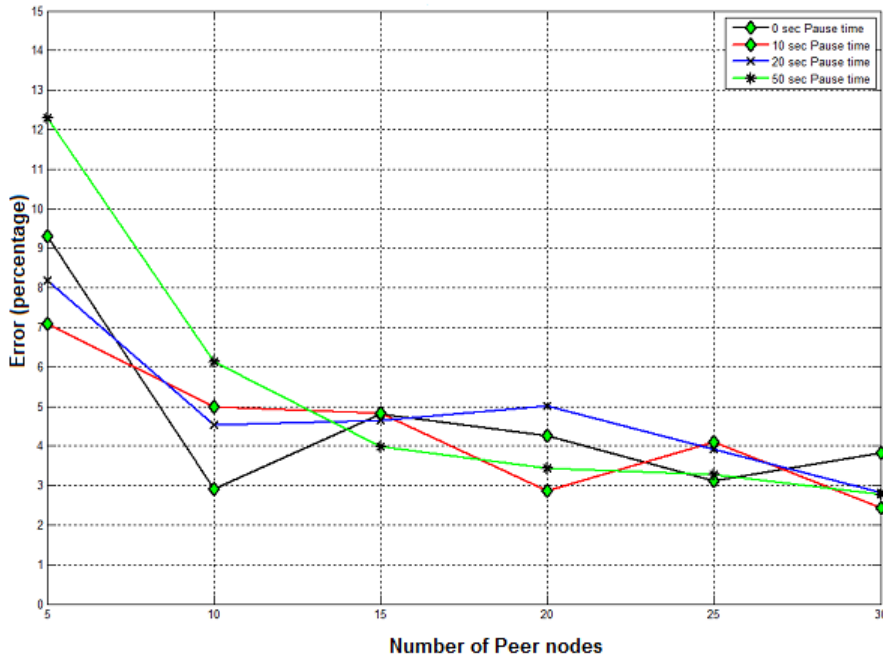


Figure 7.9: LMI with RWMM and Varying Pause time

not change, which means the target firefighter node position is constant and the peer firefighter's position is constantly changing by their movement in their respective zones.

Figure 7.11 is similar to Figure 7.10 with Error (in meter) versus number of peer nodes but this plot is generated by averaging 20 different scenarios similar to the one which generated Figure 7.10. This means that the plot is an average of 20 different target node positions inside the building. The plot clearly depicts that the accuracy of the technology does not decrease even if the target node position inside the building change. This plot proves that the position of target node inside the building does not affect the accuracy of the position technique.

Figure 7.12 is plot similar to Figure 7.11 but the range of communication is 35 m as compared to 30 m in the previous figures for firefighter mobility model. Also, in this model the building radius is 110 m which is larger than the communication range. Thus, here only a few firefighters will be in range with the target node, whereas in previous models all the firefighters inside the building were in range to the target node. From the plot we can see that the accuracy has decreased to 80% for 5 firefighters inside the building. The reason is that not all the 5 firefighters are in range

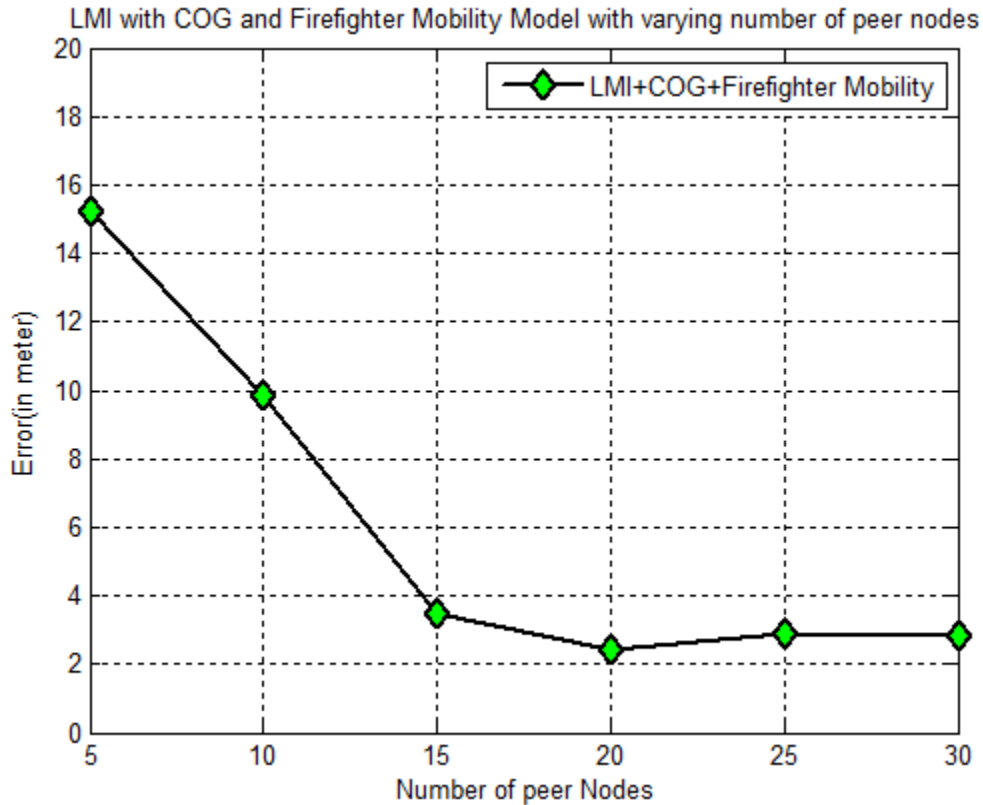


Figure 7.10: LMI with Firefighter Mobility Model and COG

and we know that the accuracy decreases significantly if the peer node count becomes less than 5. But, the accuracy of the position technique stays quite similar to previous plots as the number of firefighter increases to 10. This proves that the accuracy of technique remains constant even if the communication range is increased.

Figure 7.13 is a MatLab plot of all the peer node positions alongside real and estimated target node position. This plot is generated using real world data collected from Shelby center foyer building of Auburn University. The distances are calculated using the database from the Statistical Time-of-Arrival technique. Table of data is as shown in Table 7.1. This table depicts that the TOA distance matches the actual distance except for 5 meters which is predicted as 10 meters. In spite of having such a huge error in the distances of the peer nodes which are 5 meters away from the Target node, the accuracy of the estimated position is almost 99% with only $E = 0.55322$ meter

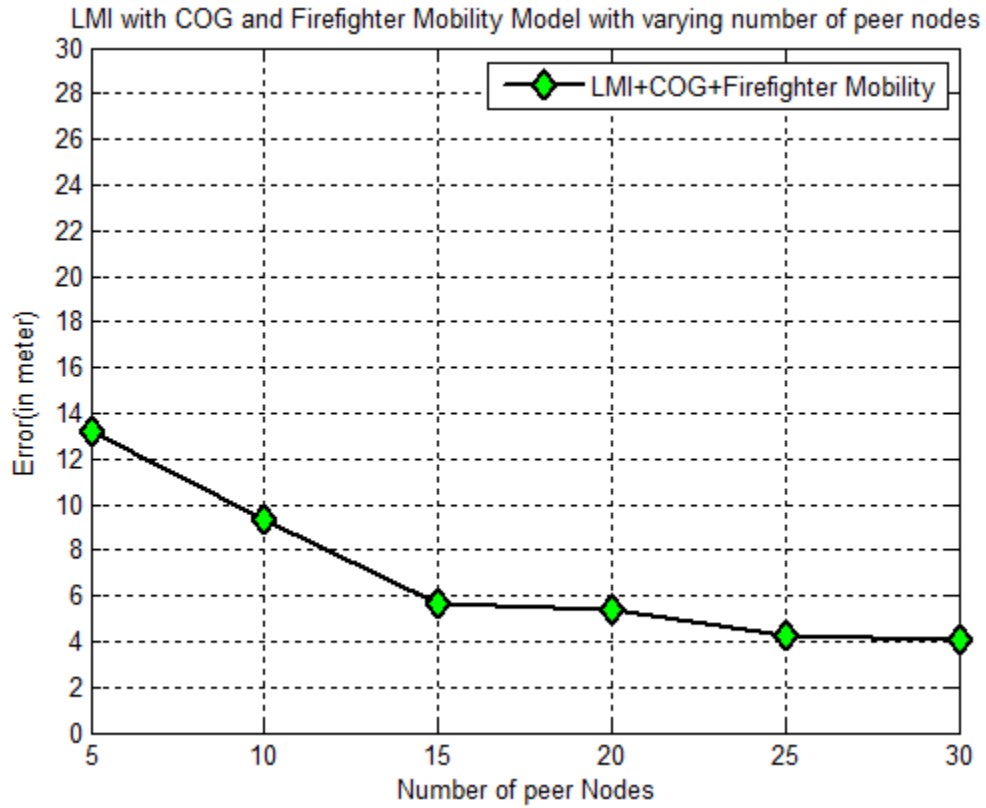


Figure 7.11: Firefighter mobility with LMI and COG along with different Target node positions

error as indicated in Figure 7.13. The indoor map of Shelby Foyer with all the nodes indicated is shown in Figure 7.14.

Node No.	X Axis	Y Axis	TOA(in meter)	Actual(in meter)
1	5	0	10	5
2	4.47	-3.175	10	5
3	2	-4.3	10	5
4	0	-10	10	10
5	3.3	9.75	10	10
6	4.35	-9	10	10
7	7.3	-6.88	10	10
8	7.4	6.7	10	10
9	3.4	-19.68	20	20
10	13.2	-15	20	20

Table 7.1: The co-ordinates are of the peer nodes and the TOA distances are obtained from Statistical TOA technique for Auburn university Shelby Foyer

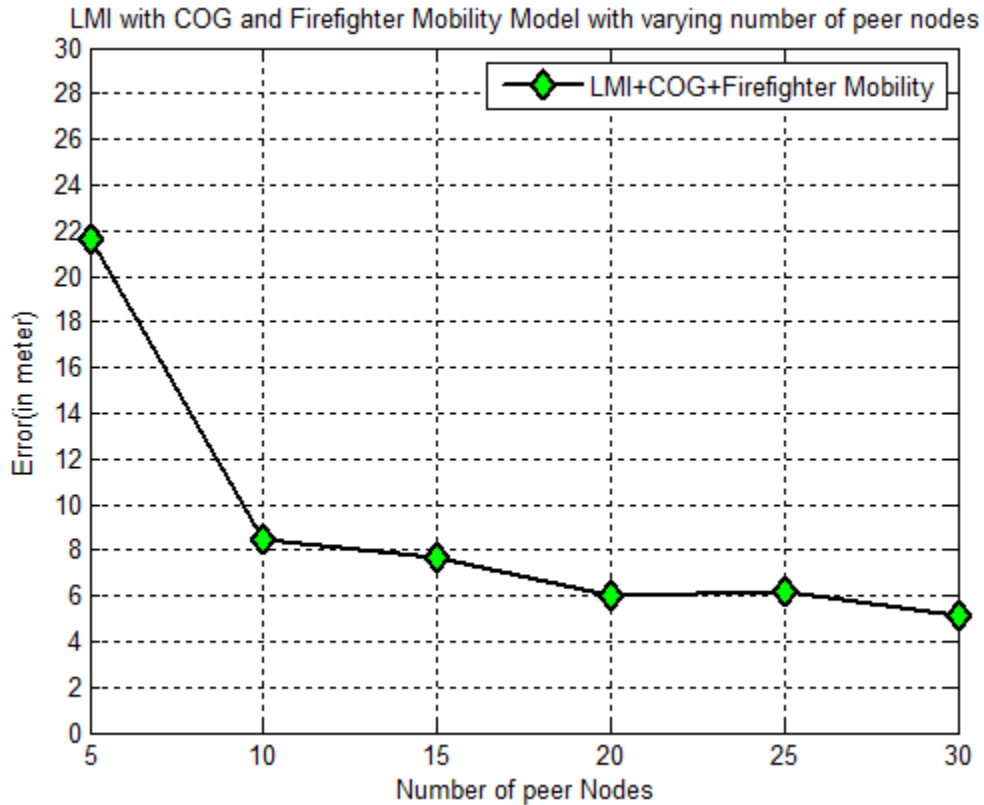


Figure 7.12: Firefighter mobility with LMI and COG along with different Target node positions and larger communication range

We conducted another experiment in the hallways of The Shelby center of Auburn University and the results are shown in Table 7.2.

Node No.	X Axis	Y Axis	TOA(in meter)	Actual(in meter)
1	5	0	10	5
2	0	-5	5	5
3	10	0	10	10
4	0	-10	10	10
5	20	0	20	20
6	0	-20	20	20
7	30	0	30	30
8	0	-30	30	30

Table 7.2: The co-ordinates are of the peer nodes and the TOA distances are obtained from Statistical TOA technique at Auburn University Shelby Center Hallway

Figure 7.15 shows the MatLab map of the Shelby center hallway with all the peer nodes, Target node and estimated target node positions. The error obtained in the estimated target node

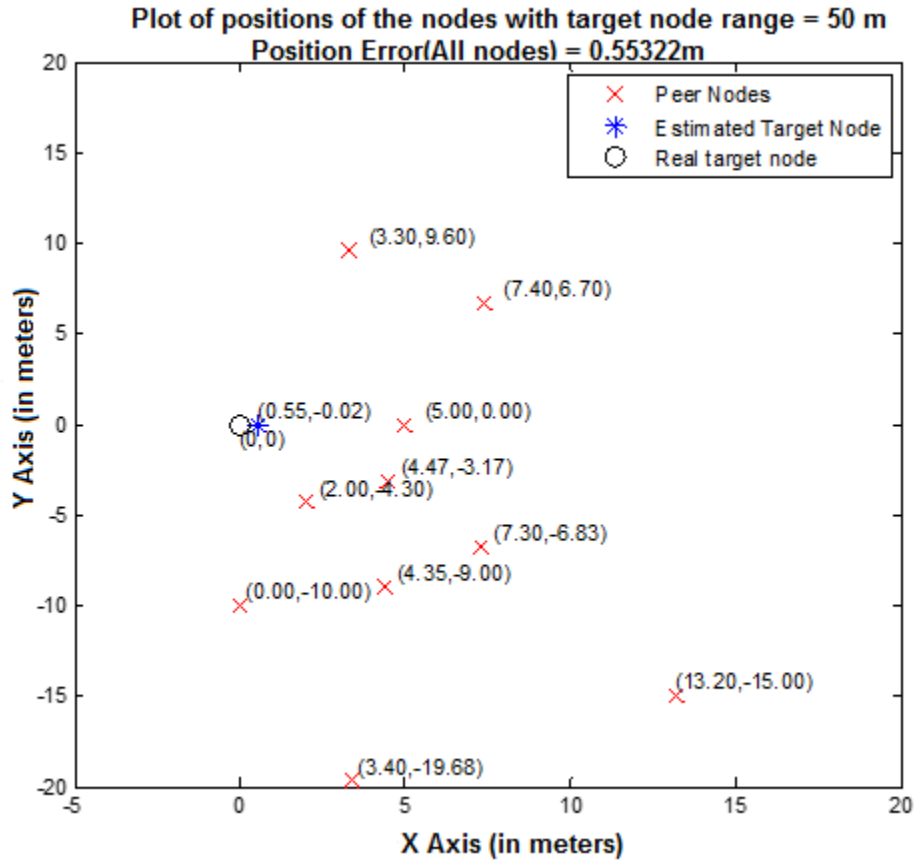


Figure 7.13: MATLAB Map of Shelby Foyer (Auburn University) including all the peer nodes, Real Target node and Estimated Target node Positions

position in this experiment is $E = 7.6537$ meters. The error in this experiment is higher as all the nodes are in a straight line and the precision of the multi-lateration dilutes similar to the case in GPS Precision Dilution of Position (PDOP) error [34].

Figure 7.16 shows the indoor map of the Shelby center Hallway (Auburn University) indicating all the peer node, target node and estimated target node position.

7.3.3 Grid Method with Center-of-Gravity

The accuracy of Grid method is better than Linear Matrix Inequality (LMI) technique in most of the cases we tested. Figure 7.17 shows that the accuracy of Grid method $E = 8.7537$ m which is higher than Linear Matrix Inequality (LMI) method $E = 12.5229$ m for same conditions on reference nodes and the same amount of error in Statistical TOA distance estimation. We conducted

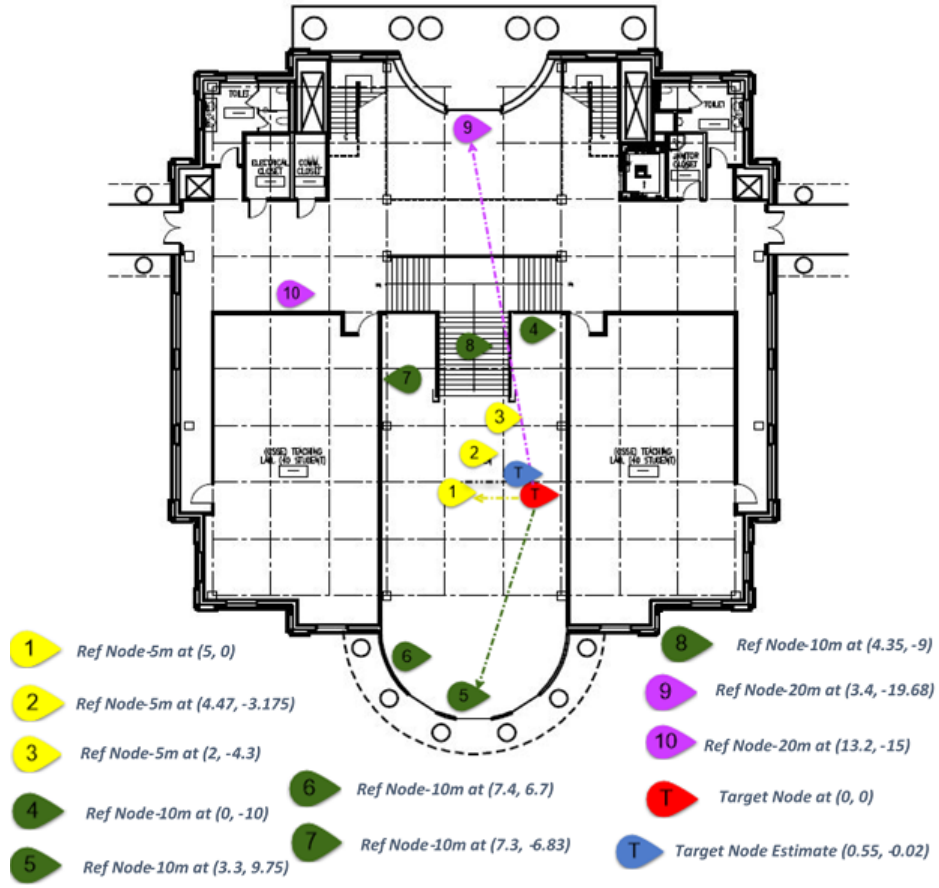


Figure 7.14: The Indoor map of Shelby Foyer (Auburn University) including all the peer nodes, Target node and estimated target node positions

many experiments to compare Linear Matrix Inequality (LMI) technique and Grid method estimation and most of the results show that Grid method provides better accuracy than LMI method. Also, LMI estimation using MatLab can run into optimization problem of infeasibility whereas we developed the Grid method to avoid such problems. Infeasibility is a condition in which the Linear Matrix inequality is not able to solve the optimization problem.

During our experiments with Grid method we found that our assumption of target node being inside the intersection area of all the reference nodes does not hold true for all the cases. In order to solve this problem we calculated the grid points of all the intersection areas which are formed by four or more reference nodes. We did not consider the intersection area of reference nodes less than four because it was satisfactory to not consider them and did not affect the grid method

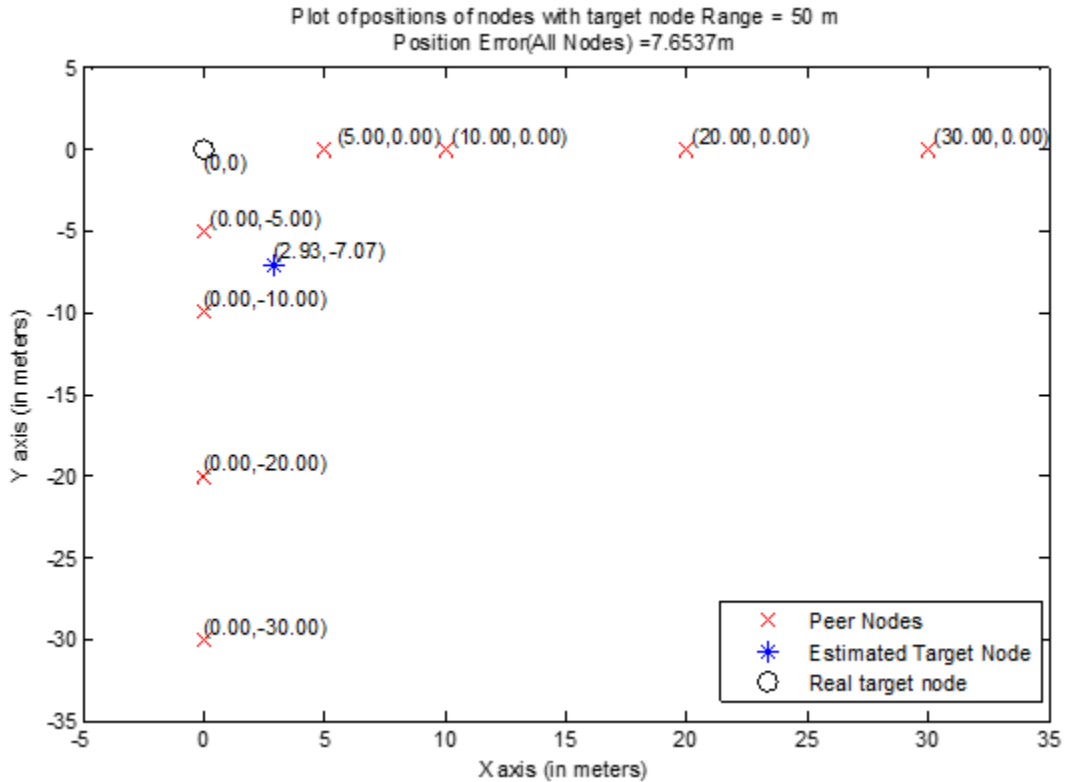


Figure 7.15: MatLab Map of Shelby Center Hallway (Auburn University) including all the peer nodes, Real Target node and Estimated Target node Positions

estimation accuracy. Also in order to reduce the error in target node estimation we implemented donut circles instead of normal circles to map the Grid Method.

Figure 7.18 shows the difference between using normal circle for communication range compared to using donut circle. The reason was to eliminate all the unnecessary grid points in the intersection area which were causing the Center-of-Gravity (COG) to move far from the real target node position which was found by numerous practical experiments.

Figure 7.19 shows the Grid points with reference node positions and donuts instead of normal circles as in Figure 5.6. It is clear from Figure 5.6 and Figure 7.19 that the numbers of grid points in Figure 7.19 is far less than number of grid points in Figure 5.6.

Figure 7.20 shows the Linear Matrix Inequality (LMI) technique and Grid method target node estimated positions and it can clearly be seen that the Grid method using donut circles is far more accurate than Linear Matrix Inequality technique. Also, the Grid method with donut is more

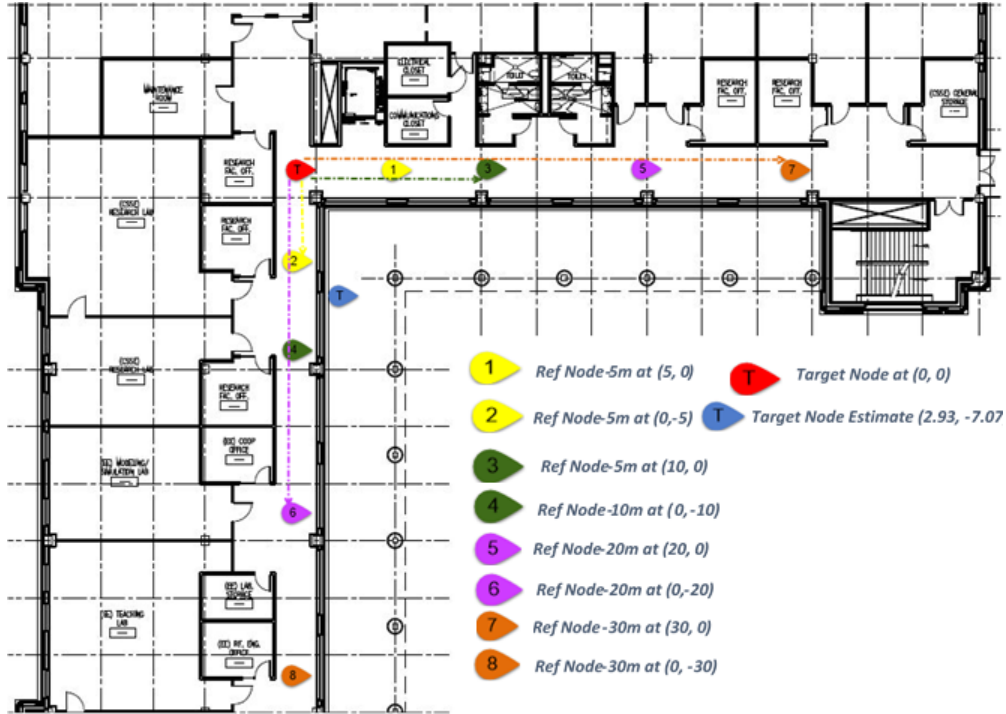


Figure 7.16: The Indoor map of Shelby Center Hallway (Auburn University) including all the peer nodes, Target node and estimated target node positions

accurate than Grid method with normal circle as its communication model. We conducted a lot of experiments to conclude that the Grid method with donut eliminates unnecessary grid points which affect the accuracy of the target node estimation.

Node no.	X Axis	Y Axis	TOA(in meter)	Actual(in meter)
1	5	0	5	5
2	0	-5	5	5
3	10	0	10	10
4	0	-10	10	10
5	20	0	20	20
6	0	-20	20	20
7	30	0	30	30
8	0	-30	30	30

Table 7.3: Table representing the Statistical TOA data for Auburn University Shelby Center hallway with Peer Reference node co-ordinates

Figure 7.21 shows the plot of reference node positions with donut circles for Auburn University Shelby Center hallway Statistical Time-of-Arrival data table as shown in Table 7.3. The different colors of Grid points represent different intersection areas depending on the number of

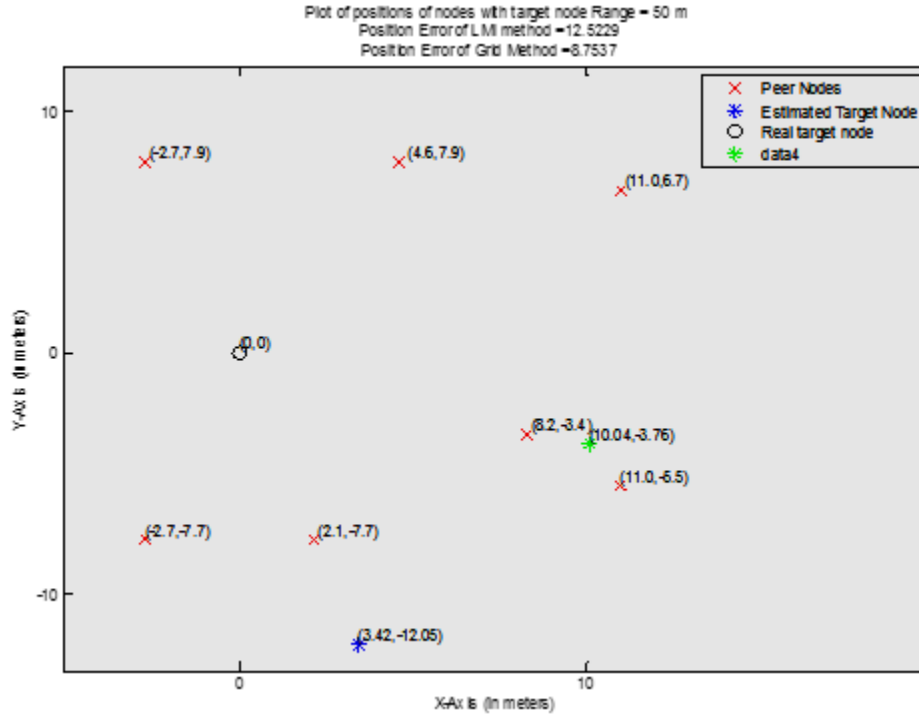


Figure 7.17: Plot of reference node position, Real Target node and Target node position estimated from Grid and LMI method

reference node donut intersections. We collected all the Grid points and provided them with appropriate weights in Center-of-Gravity (COG) calculation. We calculated the donut widths by adding and subtracting 20% of Time-of-Arrival radius from it respectively to form the lower and upper donut boundaries.

Figure 7.22 shows the plot of reference node positions with real target node and estimated target nodes from Grid method and Linear Matrix Inequality technique. It can clearly be seen that the Grid method target node estimation error is just 0.53962 meters whereas the LMI estimated target node position error is 7.6537 meters. Also, using donut circles instead of normal circles along with weighted Grid points from all the intersection areas with 4 or more intersecting donut circles we have reduced the estimation error to less than a meter.

Similarly Figure 7.23 shows the experiment in Auburn University Shelby Foyer with TOA estimated reference node distances. We can clearly see that the Grid method error is 0.060369 meters compared to 0.55322 meters from Linear Matrix Inequality technique estimation. This

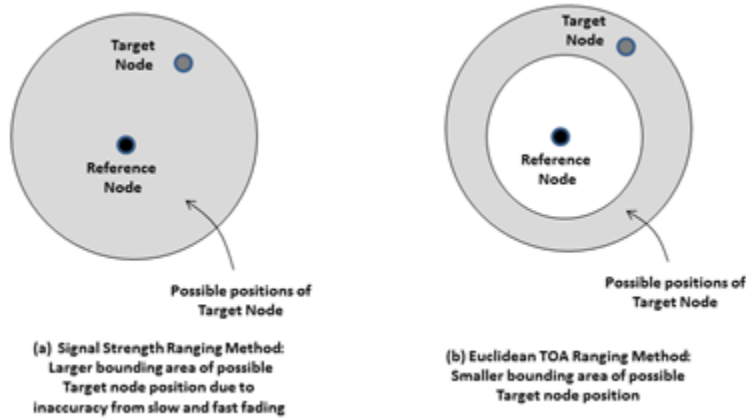


Figure 7.18: The difference between normal circle communication model and Donut circle Communication model

experiment shows that the Grid method estimation with Donut circle and weighted grid points can achieve an accuracy as high as 99%.

Figure 7.24 shows the plot similar to Figure 7.23 of Auburn university Shelby foyer but it includes the reference nodes present in different rooms. This scenario represents the non-line-of-sight (NLOS) condition as the reference nodes are placed in different rooms. The result from the experiment is the same which is the Grid method with donut and weighted Center-of-Gravity technique is better than the Linear Matrix Inequality (LMI) with Center-of-Gravity (COG) technique.

7.3.4 Comparison of Linear Matrix Inequality Technique and Grid Method for Simulation Model

In order to compare the location accuracy from Linear Matrix Inequality technique and Grid method we conducted a simulation model to generate both Linear Matrix Inequality and Grid method location for same set of reference peer node conditions. The results of these simulation results are depicted in this section.

Figure 7.25 shows the plot of number of nodes with respect to error in the Linear matrix Inequality technique and Grid method location estimation. This simulation model has reference peer nodes varying from 1 to 10 nodes in range to the target node with TOA error of 20% induced in the distance between each reference node and target node. We can clearly see that Grid method

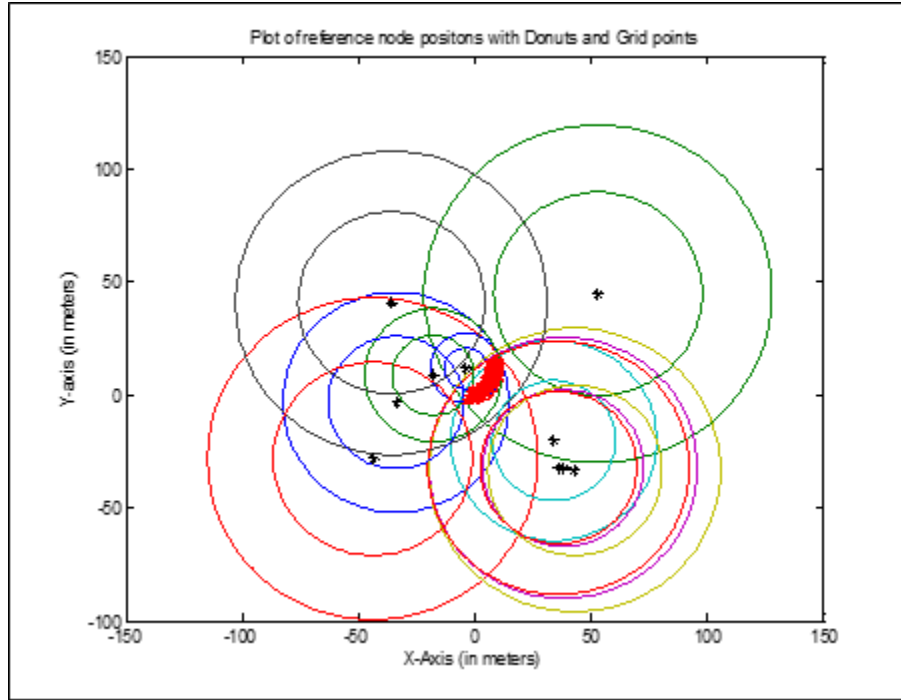


Figure 7.19: Plot of reference node positions with donuts, real target node and grid points

performs better compared to Linear Matrix Inequality technique in this condition. The reason for better performance from Grid method compared to Linear Matrix Inequality is the use of donut circles instead of normal circles for multi-lateration and Center-of-Gravity (COG) method enhancing the chance of localization accuracy.

Figure 7.26 depicts a similar graph as Figure 7.25 except for the induced error in TOA distance which is 50% instead of 20% as in Figure 7.25 simulation model. Even with 50% induced error in TOA distance between target node and each reference nodes the Grid method performs better than the Linear Matrix Inequality technique.

Figure 7.27 and Figure 7.28 depict the similar plots with 80% and 100% induced error in TOA distance respectively. All these plots conclude same result that Grid method performs better than Linear Matrix Inequality technique in all scenarios we have simulated.

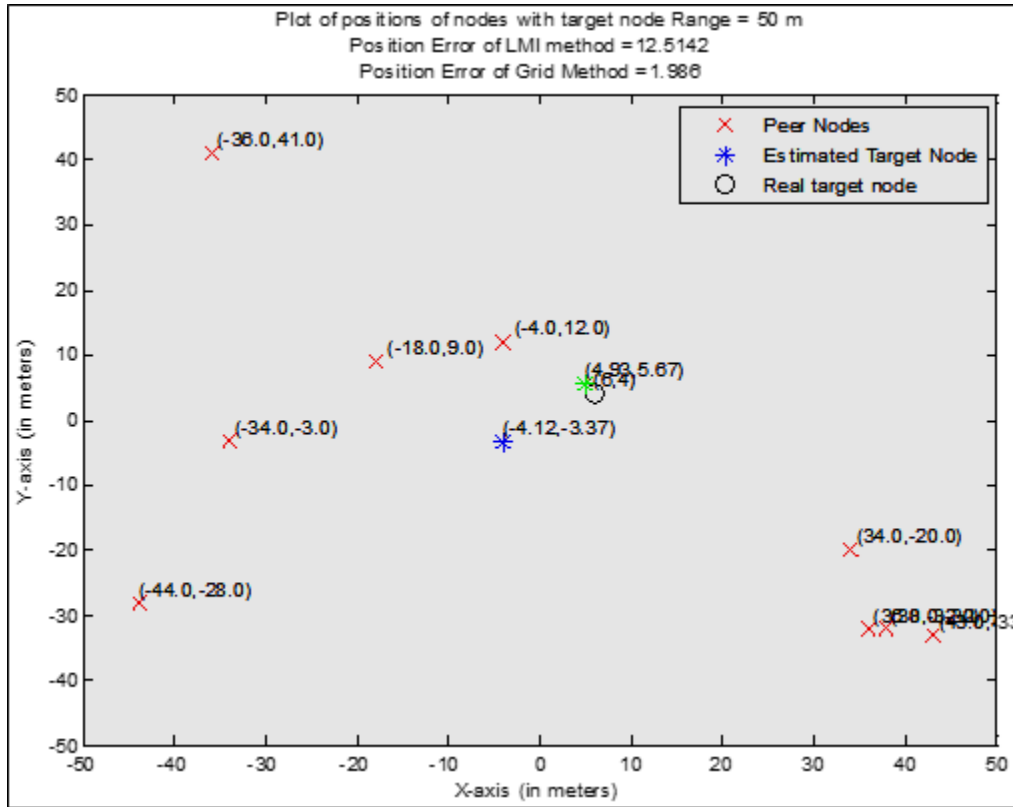


Figure 7.20: Plot of reference node positions, real target node position and target node position estimated from Grid and LMI methods

7.3.5 Comparison of Linear Matrix Inequality Technique and Grid Method for Real World Data

In Section 7.3.4 we discussed the comparison between Grid Method position estimation accuracy with that of Linear Matrix Inequality technique and in this section we will compare these techniques with real world experiment data. We conducted some experiments in different buildings of Auburn University and tabulated the Time-of-Arrival data using the Statistical Time-of-Arrival technique.

Our first experiment was conducted in Auburn University Foy Hall main floor and we collected the Time-of-Arrival samples to calculate the distance between the target node and the reference peer nodes using Statistical TOA technique. The results of the Statistical TOA technique are tabulated in Table 7.4.

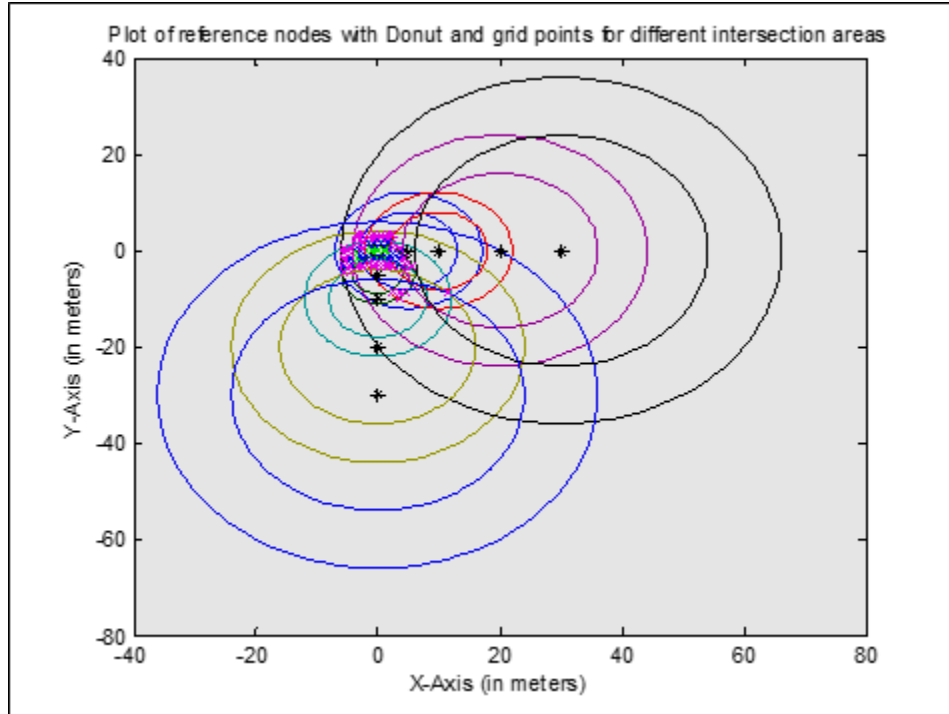


Figure 7.21: Plot of reference nodes with donuts and Grid points for different intersection areas

Node No.	X Axis	Y Axis	TOA(in meter)	Actual(in meter)
1	8.66	-5	20	10
2	-8	6	-	10
3	18.73	7	20	20
4	-13.22	-15	20	20
5	29.17	7	30	30
6	25.98	15	30	30

Table 7.4: Table representing the Statistical TOA data for Auburn University Foy Hall Main Floor with Peer Reference node co-ordinates

It can be seen from Table 7.4 that all the reference peer node distances have been correctly estimated except for node 1 which is estimated as 20 meters instead of 10 meters and distance of node 2 is not estimated at all. So, we eliminated node 2 from our calculation which brings the number of reference peer node to $N = 5$. The Grid method with weighted Center-of-Gravity position estimation error for the data in Table 7.4 is 4.88 meters compared to 7.77 meters of Linear Matrix Inequality technique.

Figure 7.29 shows a MatLab plot of target node position estimation for both Linear matrix Inequality (LMI) technique as well as Grid method for statistical Time-of-Arrival (TOA) data

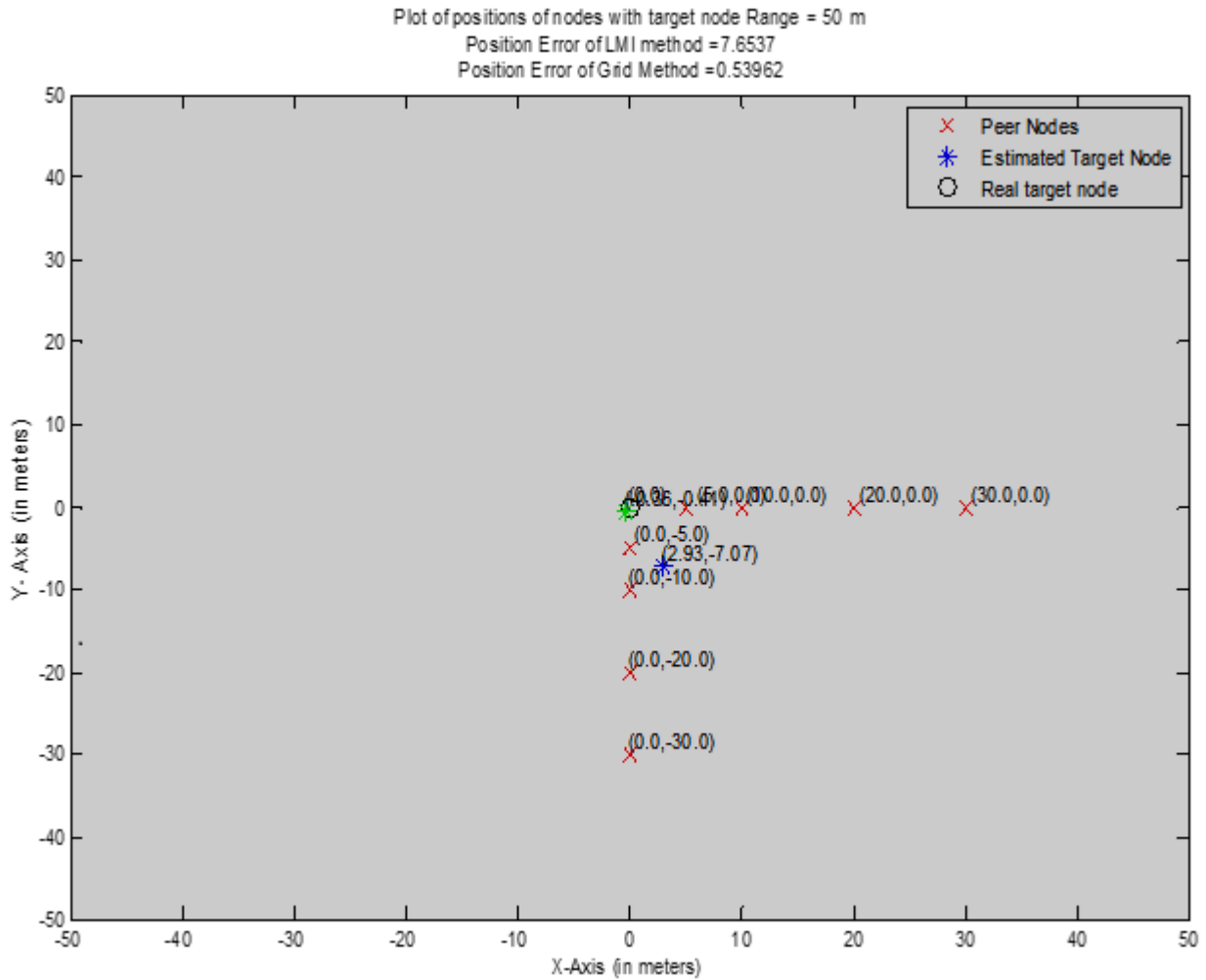


Figure 7.22: Plot of Reference node positions, Real target node and estimated target node position from Grid and LMI method for Auburn University Shelby Hallway

of Table 7.4 of Auburn University Foy Hall main floor. It also indicates all the reference node positions on the plot.

Our second experiment was conducted in multiple rooms of Auburn University Shelby center and we collected samples similar to our precious experiment in Foy Hall of Auburn University. All the data has been tabulated into Table 7.5 after performing Statistical TOA technique to obtain the distances between the reference peer nodes and the Target node.

We see from Table 7.5 that the actual distance are not exact as the database distances in order to match them using the Statistical TOA technique, but still the technique produced better results. The Grid method with weighted Center-of-Gravity technique position estimation error is

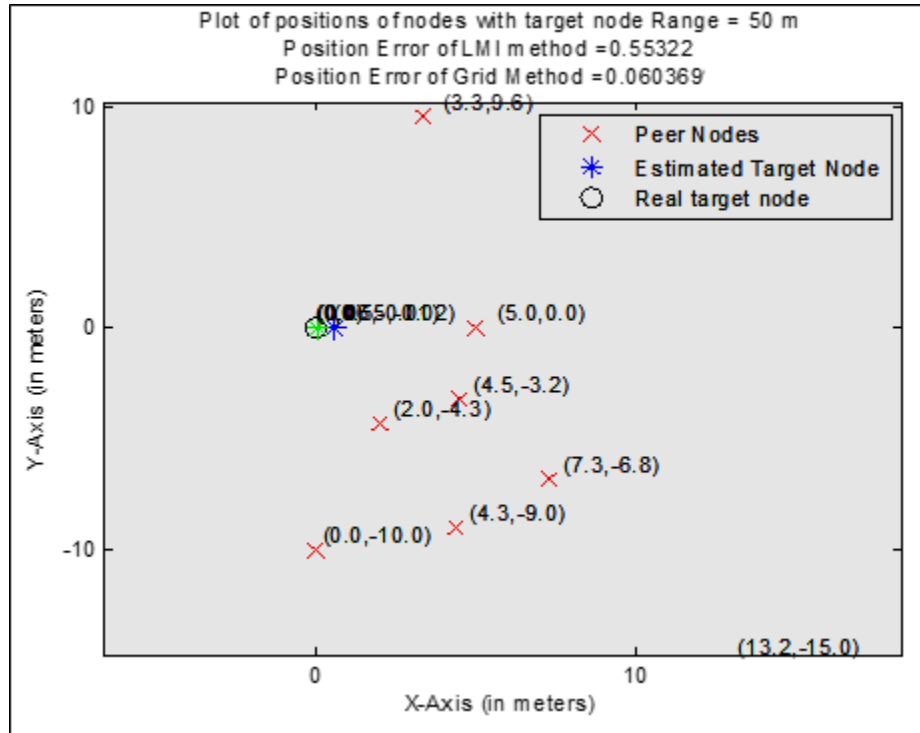


Figure 7.23: Plot of reference node positions, real Target node position and estimated target node position from Grid and LMI methods for Auburn University Shelby Foyer

Node No.	X Axis	Y Axis	TOA(in meter)	Actual(in meter)
1	11.84	9.53	20	15.19
2	15.39	9.53	20	18.10
3	20.57	9.53	30	22.67
4	26.36	9.53	20	28.03
5	30.93	9.53	30	32.36
6	-6.78	9.53	10	11.69
7	8.99	3.89	10	9.79
8	8.99	-2.74	20	9.40
9	-5.24	-3.96	10	6.57

Table 7.5: Table representing the Statistical TOA data for Multiple rooms of Auburn University Shelby Center hallway and multiple rooms with Peer Reference node co-ordinates

only 1.292 meters whereas the Linear Matrix Inequality technique was infeasible and could not provide any location for the Target node.

Figure 7.30 shows a MatLab plot of target node position estimation for both Linear matrix Inequality (LMI) technique as well as Grid method for statistical Time-of-Arrival (TOA) data of

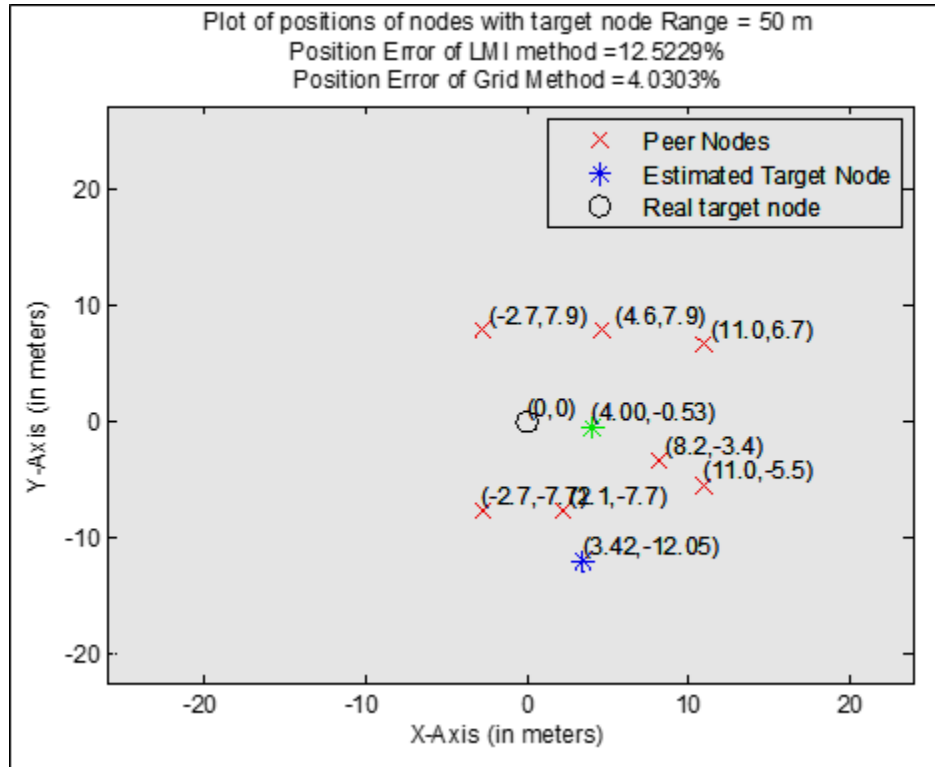


Figure 7.24: Plot of reference node positions, real Target node position and estimated target node position from Grid and LMI methods for Auburn University Hallway and multiple rooms

Table 7.5 of Auburn University Shelby Center hallway and multiple rooms. The plot also includes the reference node positions.

Similar to the second experiment we conducted another experiment in the multiple rooms of Auburn University Shelby Center. Table 7.6 shows the data collected from the experiment along with the Statistical TOA technique distance estimation between target node and reference peer node.

Node No.	X Axis	Y Axis	TOA(in meter)	Actual(in meter)
1	3.048	9.525	10	10
2	8.992	3.886	30	9.79
3	-3.0226	9.252	10	10
4	-8.890	-4.572	10	10
5	-6.833	7.6962	10	10.29
6	-3.023	19.761	30	20

Table 7.6: Table representing the Statistical TOA data for Multiple rooms of Auburn University Shelby Center with Peer Reference node co-ordinates

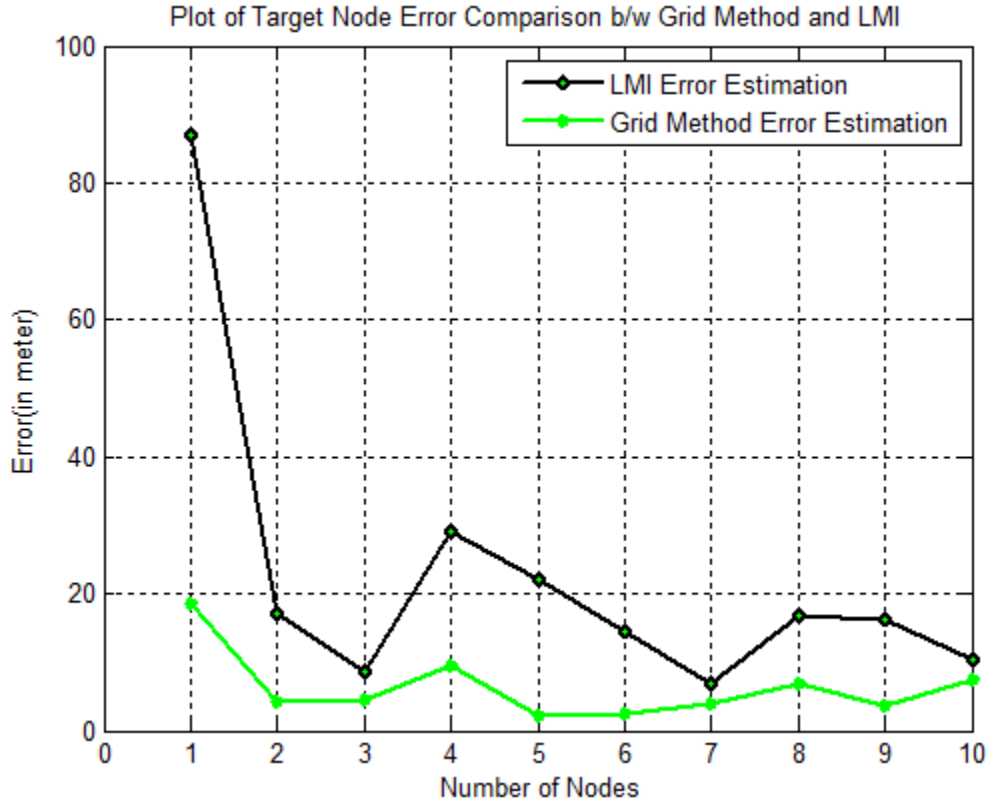


Figure 7.25: Plot of target node location error comparison between LMI and Grid method with 20% induced TOA distance error.

From Table 7.6 it can clearly be seen that most of the results from the Statistical TOA technique match to the actual distance except node 2 and node 6. The Grid Method with weighted Center-of-Gravity technique position estimation error for the data from Table 7.6 is 1.42 meters compared to 4.70 meters of Linear Matrix Inequality technique.

Figure 7.31 shows a MatLab plot of target node position estimation for both Linear matrix Inequality (LMI) technique as well as Grid method for statistical Time-of-Arrival (TOA) data of Table 7.6 of Auburn University Shelby Center hallway and multiple rooms. The plot also indicates all the reference node co-ordinates along with the estimated Target node positions.

Our fourth experiment was conducted in the Auburn University Broun Hall second floor. All the data has been tabulated in Table 7.7.

The distance between target node and the reference node is calculated using the Statistical Time-of-Arrival technique. The Grid Method with weighted Center-of-Gravity technique position

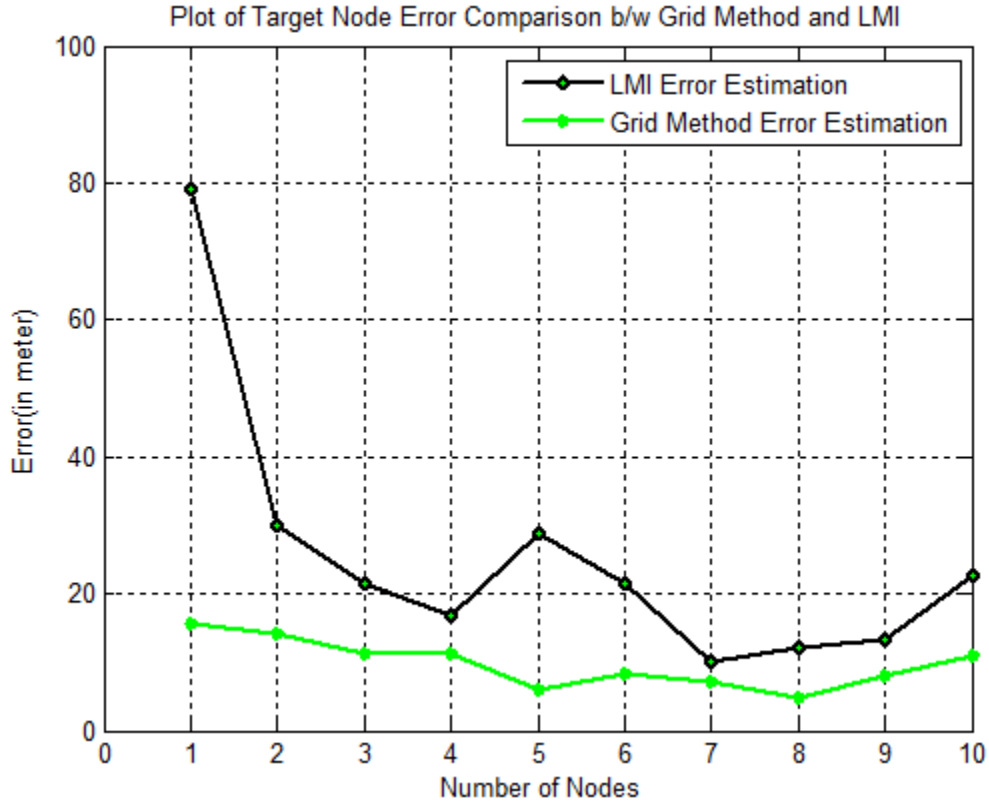


Figure 7.26: Plot of target node location error comparison between LMI and Grid method with 50% induced TOA distance error.

Node No.	X Axis	Y Axis	TOA(in meter)	Actual(in meter)
1	-5.18	-7.93	10	9.47
2	-5.18	-17.38	20	18.13
3	-3.35	-17.98	30	18.29
4	-5.18	10.36	10	11.59
5	0.61	17.68	30	17.69
6	-14.33	0	30	14.33
7	-15.70	5.18	30	16.53
8	-31.24	1.63	30	31.28
9	6.10	3.36	10	6.96
10	6.10	-3.36	20	6.96

Table 7.7: Table representing the Statistical TOA data for Multiple rooms of Auburn University Shelby Center with Peer Reference node co-ordinates

estimation error is 0.3536 meters compared to 3.5202 meters error of Linear Matrix Inequality technique.

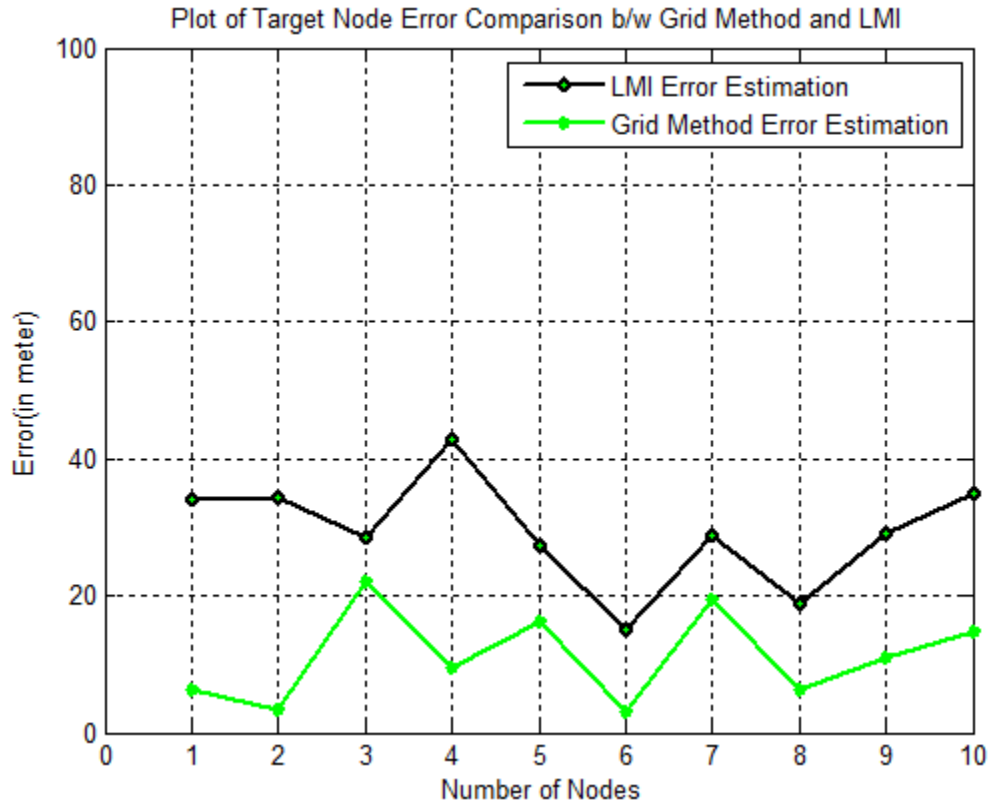


Figure 7.27: Plot of target node location error comparison between LMI and Grid method with 80% induced TOA distance error.

Figure 7.32 shows a MatLab plot of target node position estimation for both Linear matrix Inequality (LMI) technique as well as Grid method for statistical Time-of-Arrival (TOA) data of Table 7.7 of Auburn University Broun hall second floor. It also indicates all the reference node positions on the plot along with estimated target node positions.

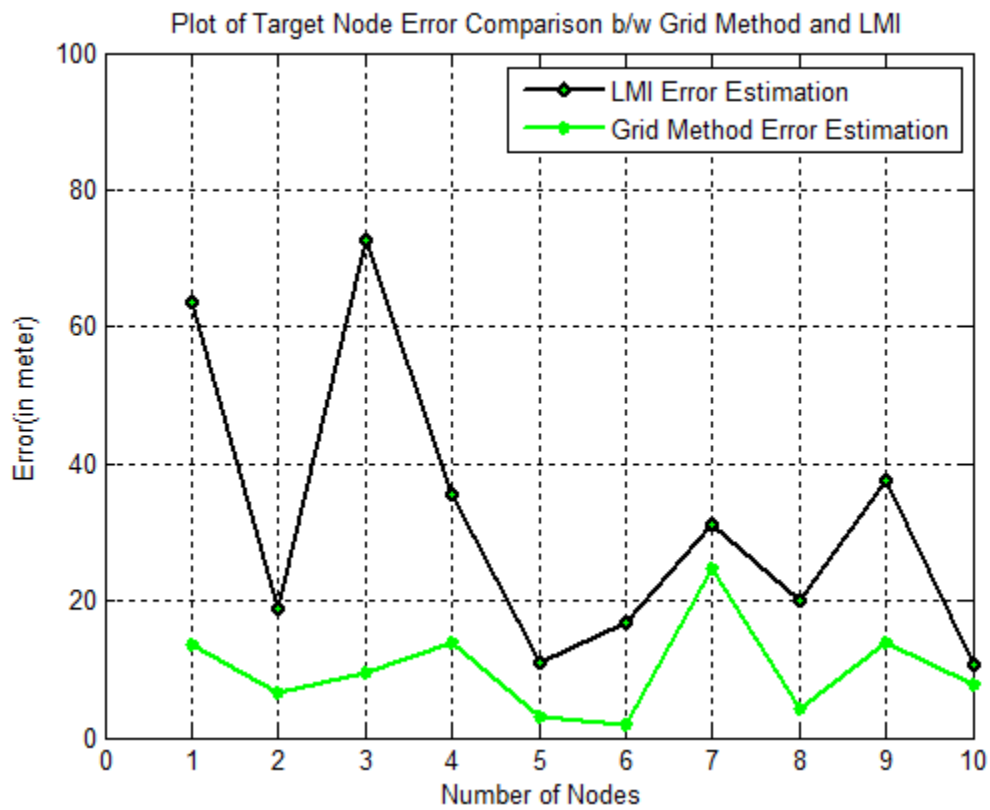


Figure 7.28: Plot of target node location error comparison between LMI and Grid method with 100% induced TOA distance error.

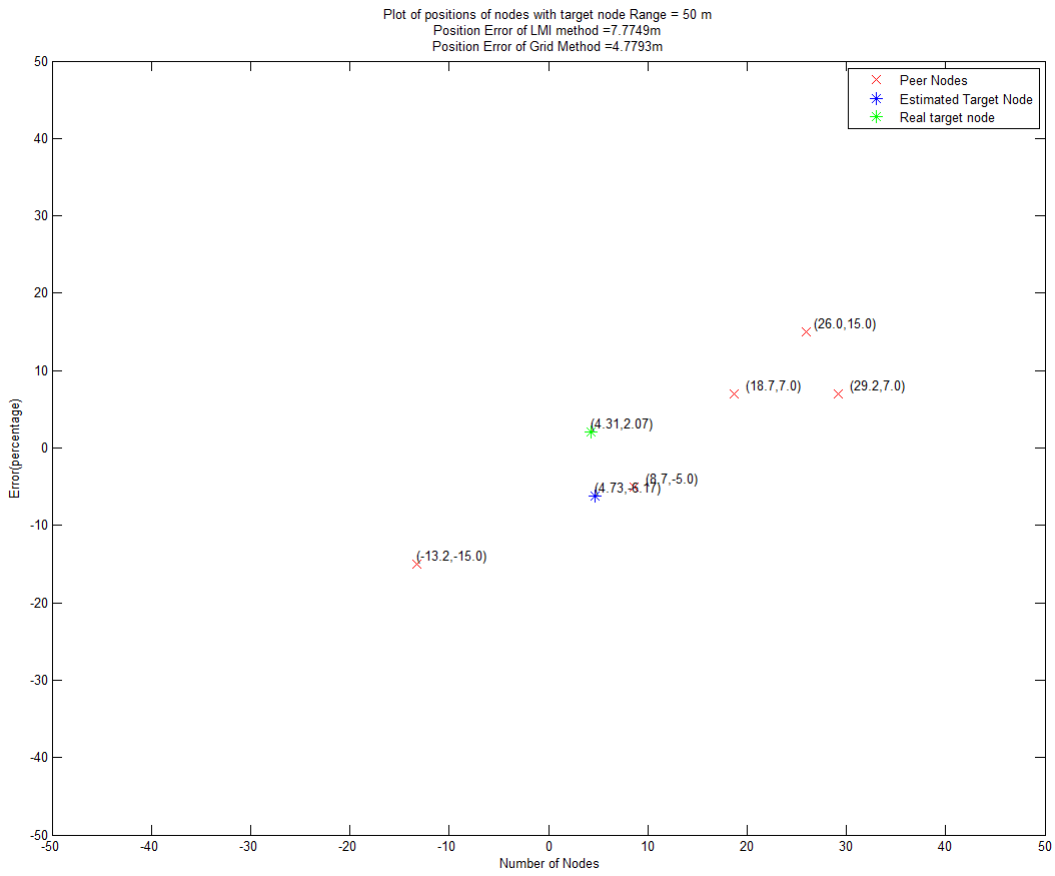


Figure 7.29: Plot of target node location error comparison between LMI and Grid method for Statistical TOA data for Auburn University Foy Hall Main Floor

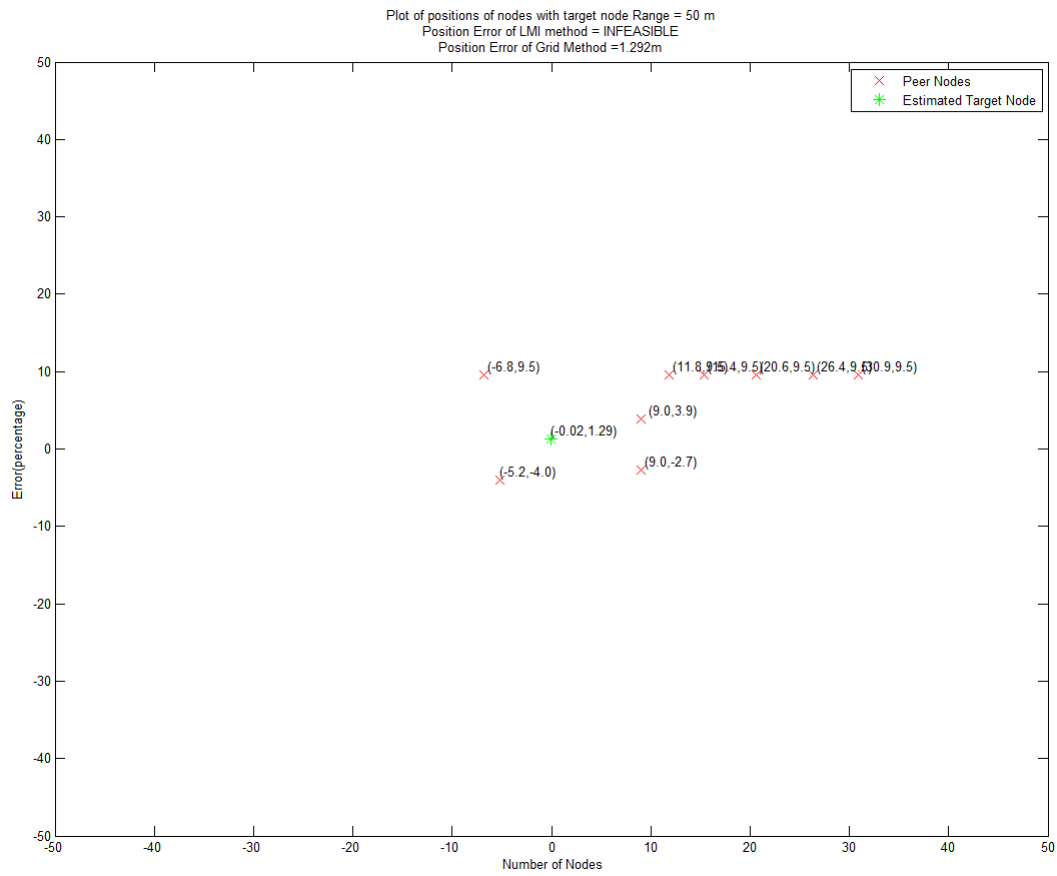


Figure 7.30: Plot of target node location error comparison between LMI and Grid method for Statistical TOA data for Auburn University Shelby center hallway and multiple rooms.

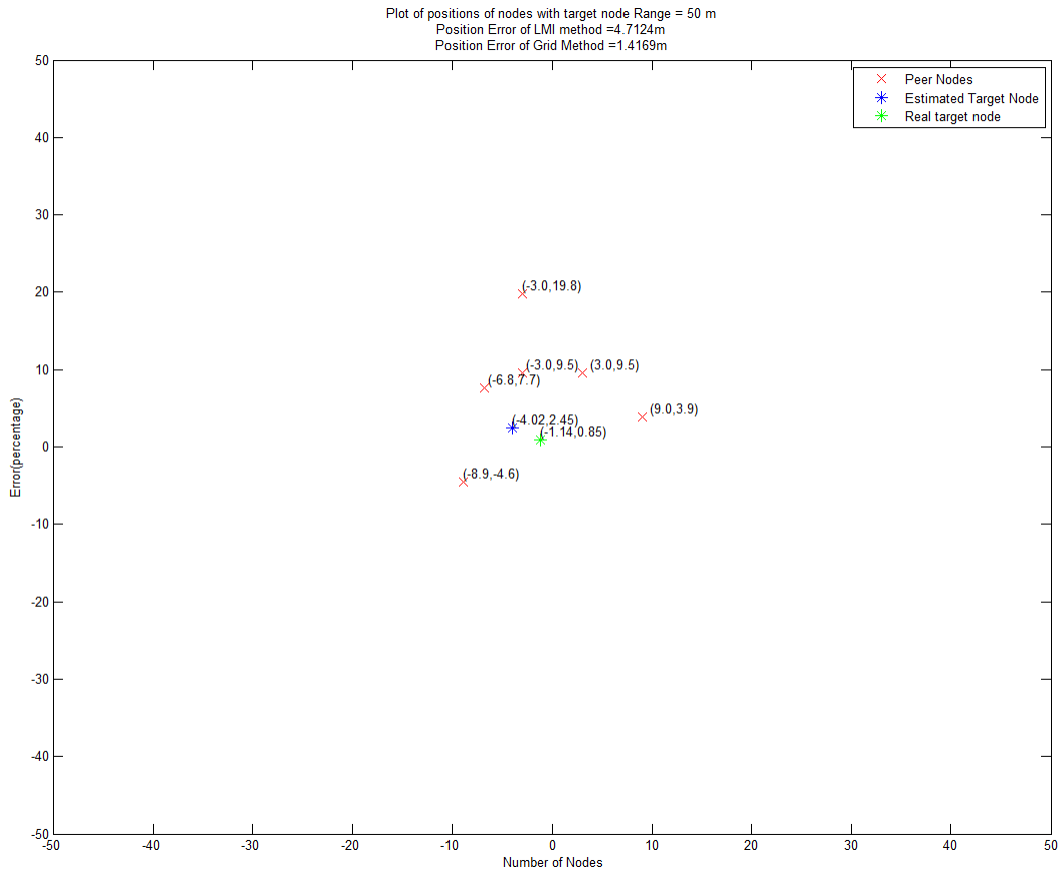


Figure 7.31: Plot of target node location error comparison between LMI and Grid method for Statistical TOA data for Auburn University Shelby center hallway and multiple rooms.

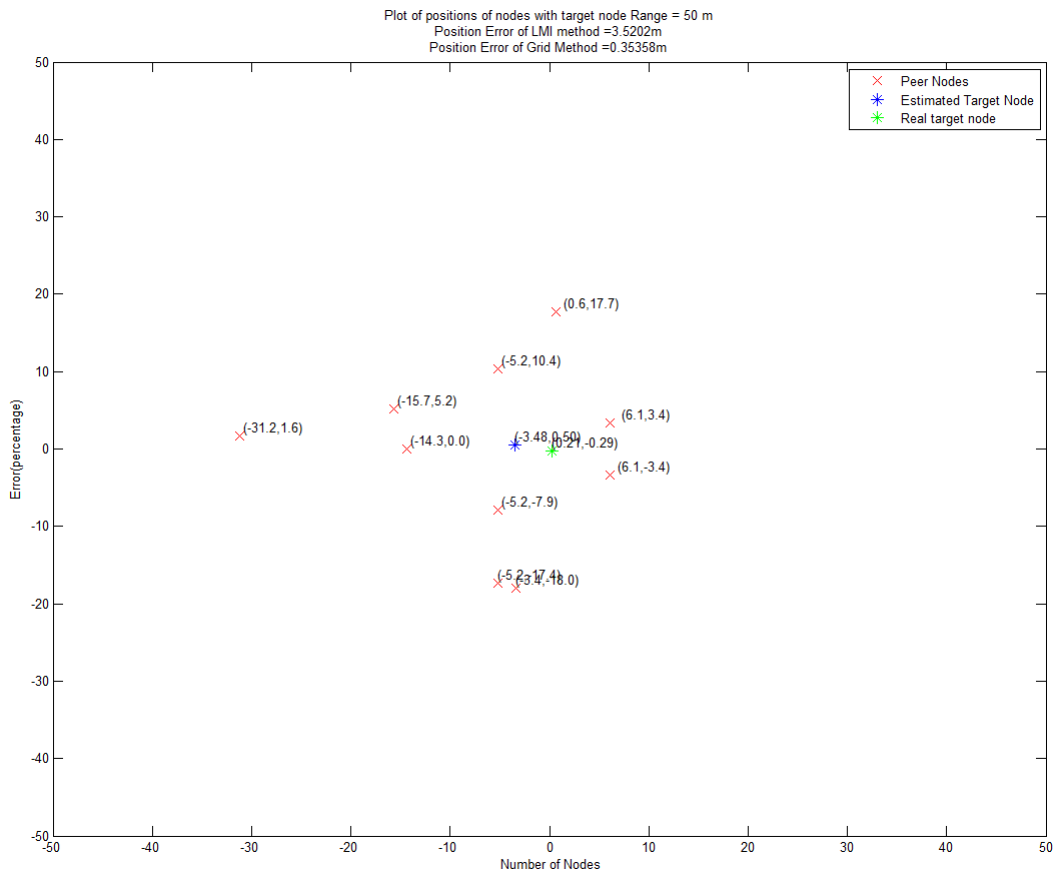


Figure 7.32: Plot of target node location error comparison between LMI and Grid method for Statistical TOA data for Auburn University Broun hall Second floor.

8.1 Conclusion

We propose an algorithm in which a target node (user) infers localization information using the positions of other passing-by nodes (peers) and approximate range information. The interaction between target node and peer reference nodes is modeled by considering several parameters that permit us to compare the performance in different scenarios. Also, we have proposed, implemented and evaluated a self-localization technology using three techniques which are Statistical Time-of-Arrival (TOA) technique, Linear Matrix Inequality (LMI) or Grid Method and Center-of-gravity (COG). The Statistical Time-of-Arrival (TOA) is the first stage of the localization technology which collects the Round-Trip-Time (RTT) for each reference nodes and calculates the distance between the target node and the peer reference nodes. The second stage consists of Linear Matrix Inequality (LMI) or Grid Method to estimate the target node position using the distance and peer reference node position co-ordinates collected from the first stage. The Center-of-Gravity (COG) technique constitutes the third stage of the technology which improves the accuracy by collect a cluster of target node positions and calculating the COG of the cluster.

The contributions of our work includes the following :

- Inclusion of Time-Of-Arrival (TOA) ranging technique to obtain a better accuracy and reliability compared to other ranging techniques such as RSSI, etc.
- Design of a low-cost, simple Self-localization technology for indoor localization and navigation.
- Improvement of accuracy by incorporating Center-of-Gravity (COG) technique.

The accuracy of the self-localization technology for early simulation experiments is as follows: During the study we obtained a localization accuracy of 90% using Linear Matrix Inequality (LMI) for just 10 reference peer nodes within range of the user even though the range error obtained from the Euclidean Time-of-Arrival(TOA) method was 20%. This localization accuracy increased to 97% when the number of in-range reference peer nodes is increased to 200, which is a very spectacular achievement as the range estimation error is very high compared to the localization error. The duty cycle of the opportunistic scan phase has been observed to have a significant impact on the user self-positioning estimation, i.e. the shorter the duty cycle the less the rendezvous probability with peers and, in turn, the lower the localization accuracy. Furthermore, we observed that the proposed opportunistic localization scheme is rather robust to the self-positioning error model for peers. In fact, the correlation, the standard deviation and the drift of the self-positioning error do not significantly affect the localization accuracy, provided that the algorithm is performed over the data gathered with a large enough number of opportunistic exchanges (large number of peers).

After the early simulation experiments we developed a new Statistical Time-of-Arrival (TOA) to replace the erroneous Euclidean Time-of-Arrival (TOA) technique. The Statistical TOA technique provided a better accuracy with most of the peer nodes providing a 100% accuracy. Also, we developed a new technique known as Grid Method which replaced the Linear Matrix Inequality (LMI) technique as it used Matlab software for its calculation. During the study we obtained a localization accuracy of less than a meter for just 5 reference peer nodes within range of the target node even though the range error obtained from the Statistical Time-of-Arrival (TOA) method was high for some peer reference nodes, which makes it perfect for indoor tracking and navigation. Also, these experiments included real world data compared to simulation data in the earlier experiments which provides a strong proof of the working of the device in real-world scenarios. Also we have developed and tested various mobility models to test the reliability of our technology when all the nodes are mobile.

We have achieved a sub-meter accuracy without incorporating any special hardware such as Ultra-Wideband(UWB) or any complex techniques. Our technology is simple low-cost and reliable in all the experiments proposed in this thesis.

8.2 Future Work

There are many possibilities for the future work in the area of Self-localization of target nodes. Our future work involves developing simulation models for cases where all devices in an area are deprived of GPS location information, which leads to a condition where only relative localization of all the devices in the network is possible and can be obtained by using opportunistic self-localization scheme discussed in the thesis. This model can be employed in offices and in warehouses, where relative positions are useful for object location and tracking applications are possible with large-scale ad-hoc networks of wireless tags. Also, another possibility is to develop a device which can provide localization to lost firefighters inside the fire scene which improves the safety of the firefighters. The device needs to be rugged to handle all the harsh environments in which firefighters perform their tasks.

Bibliography

- [1] J. Albowicz, A. Chen, and L. Zhang. “Recursive position estimation in sensor networks”. In: *Proc. of the 9th International Conference on Network Protocols (ICNP 2001)*. Riverside, CA, USA, 2001, pp. 35–41.
- [2] Daniel C. Asmar, John S. Zelek, and Samer M. Abdallah. “SmartSLAM: localization and mapping across multienvironment”. In: *Proc. of the 2004 IEEE International Conference on Systems, Man and Cybernetics*.
- [3] Jonathan Bachrach and Christopher Taylor. *Localization in sensor networks*.
- [4] A. Boukerche et al. “Enlightness: An enhanced and lightweight algorithm for timespace localization in wireless sensor networks”. In: *Proc. of the 13th IEEE Symposium on Computers and Communications (ISCC)*. 2008, pp. 1183–1189.
- [5] Azzedine Boukerche et al. “Localization Systems for Wireless Sensor Networks”. In: *Proceedings of the 2007 IEEE Wireless Communications*. 2007.
- [6] Peter Brida et al. “A new Complex Angle of Arrival location method for ad hoc networks”. In: *Proceedings of 7th Workshop on Positioning Navigation and Communication (WPNC)*. 2010, pp. 284–290.
- [7] J. Broch et al. “A performance comparison of multi-hop wireless ad hoc network routing protocols”. In: *Proc. of the Fourth Annual ACM/IEEE International Conference on Mobile Computing and Networking (Mobicom98)*. 1998.
- [8] N. Bulusu, J. Heidemann, and D. Estrin. “Gps-less low cost outdoor localization for very small devices”. In: *Proceedings of IEEE Personal Communications Magazine*. 2000, pp. 28–34.

- [9] Darius Burschka and Gregory D. Hager. “V-GPS(SLAM): Vision-Based Inertial System for Mobile Robots”. In: *Proceedings of the 2004 IEEE International Conference on Robotics and Automation*. New Orleans, LA, 2004.
- [10] Ciprian-Romeo ComUa et al. “Wireless Localization using Time Difference of Arrival in Narrow-Band Multipath Systems”. In: *Proceedings of International Symposium on Signals, Circuits and Systems*. 2007, pp. 1–4.
- [11] Jonathan Dixon and Oliver Henlich. *Mobile Robot Navigation*. 1997. URL: http://www.doc.ic.ac.uk/~nd/surprise_97/journal/vol4/jmd/.
- [12] L. Doherty, L. E. Ghaoui, and K. S. J. Pister. “Convex position estimation in wireless sensor networks”. In: *Proc. of IEEE INFOCOM*. 2001, pp. 1655–1663.
- [13] *Driverless Car Market Watch*. URL: <http://www.driverless-future.com/>.
- [14] H. Elkachouchi and M. Abd elsalam Mofeed. “Direction-of-arrival methods (DOA) and time difference of arrival (TDOA) position location technique”. In: *Proceedings of the Twenty-Second National Radio Science Conference*. 2005, pp. 173–182.
- [15] F. Evennou and F. Marx. “Advanced integration of wifi and inertial navigation systems for indoor mobile positioning”. In: (2001), pp. 1–11.
- [16] D. Fagan and R. Meier. “Intelligent time of arrival estimation”. In: *Proceedings of IEEE Integrated and Sustainable Transportation System (FISTS)*. 2011, pp. 60–66.
- [17] D. Fox et al. “A probabilistic approach to collaborative multi-robot localization”. In: *Autonomous Robots*. 2000, pp. 325–344.
- [18] Douglas J. Geiger. “High Resolution Time Difference of Arrival Using Timestamps for Localization in 802.11b/g Wireless Networks”. In: *Proceedings of IEEE Wireless Communication and Networking Conference*. 2010, pp. 1–6.

- [19] Christian Gentner and Thomas Jost. “Indoor positioning using time difference of arrival between multipath components”. In: *Proceedings of Indoor Positioning and Indoor Navigation (IPIN)*. 2013, pp. 1–10.
- [20] J. Gonzalez et al. “Localización de vehículos combinando tecnología UWB y Gps en entornos interiores y exteriores”. In: *Proceedings of IEEE XVIII Jornadas de Automatica, Huelva*. 2007.
- [21] Kai He et al. “A Hybrid Indoor Positioning System Based on UWB and Inertial Navigation”. In: *Proceedings of IEEE Wireless Communications and Signal Processing*. 2015, pp. 1–5.
- [22] T. He et al. “Range-free localization schemes for large scale sensor networks”. In: *Proc. of the 9th Annual International Conference on Mobile computing and networking (MobiCom)*. 2003, pp. 81–95.
- [23] A. Howard, M. Mataric, and G. Sukhatme. “Localization for mobile robot teams using maximum likelihood estimation”. In: *Proc. of the IEEE/RSJ International Conference on Intelligent Robots and System (IROS)*. 2002, pp. 434–439.
- [24] R. Huang and G. V. Zaruba. “Static path planning for mobile beacons to localize sensor networks”. In: *Proc. of the 5th Annual IEEE International Conference on Pervasive Computing and Communications Workshops (PerCom Workshops 2007)*. White Plains, NY, USA, 2007, pp. 323–330.
- [25] Mathworks Inc. *Robust Control Toolbox*. URL: http://www.mathworks.com/help/robust/index.html?s_cid=doc_ftr&requestedDomain=www.mathworks.com.
- [26] Fernán Izquierdo et al. “Performance evaluation of a TOA-based trilateration method to locate terminals in WLAN”. In: (2006).
- [27] Philippe Jacquet et al. “Optimized Link State Routing Protocol for Ad Hoc Networks”. In: *Proceedings of IEEE International Multi Topic Conference*. Lahore, Pakistan, 2001.

- [28] *Linear Programming*. URL: https://en.wikipedia.org/wiki/Linear_programming.
- [29] Charles Little and Ralph Peters. “Simulated Mobile Self-Location Using 3D Range Sensing and an A-Priori Map”. In: *Proceedings of the 2005 IEEE International Conference on Robotics and Automation*. Barcelona, Spain, 2005.
- [30] Bodhibrata Mukhopadhyay, Sanat Sarangi, and Subrat Kar. “Performance Evaluation of Localization Techniques in Wireless Sensor Networks Using RSSI and LQI”. In: *Proceedings of Twenty First National Conference on Communications (NCC)*. 2015, pp. 1–6.
- [31] N. Patwari, R. O’Dea, and Y. Wang. “Relative location in wireless networks”. In: *Proc. of the IEEE VTS 53rd Vehicular Technology Conference(VTC)*. 2001, pp. 443–451.
- [32] N. Patwari et al. “Locating the nodes: cooperative localization in wireless sensor networks”. In: *Proceedings of IEEE Signal Processing Magazine*. 2005, pp. 54–69.
- [33] Pengfei Peng et al. “A cooperative target location algorithm based on time difference of arrival in wireless sensor networks”. In: *Proceedings of International Conference on Mechatronics and Automation*. 2009, pp. 696–701.
- [34] *Position Dilution of Precision (PDOP)*. URL: http://manuals.deere.com/omview/OMPC21120_19/OUO6050_000227B_19_22AUG07_1.htm.
- [35] S. Roumeliotis and G. Bekey. “Collective localization: a distributed kalman filter approach to localization of groups of mobile robots”. In: *Proc. of the 2000 IEEE International Conference on Robotics and Automation (ICRA)*. 2000, pp. 2958–2965.
- [36] C. Savarese, J. M. Rabaey, and K. Langendoen. “Robust positioning algorithms for distributed ad-hoc wireless sensor networks”. In: *Proc. of the 2002 USENIX Annual Technical Conference*. San Francisco, CA, USA, 2002, pp. 317–327.
- [37] A. Savvides, H. Park, and M. B. Srivastava. “The bits and flops of the n-hop multilateration primitive for node localization problems”. In: *Proc. of the 1st ACM international workshop on wireless sensor networks and applications(WSNA)*. 2002, pp. 112–121.

- [38] A. Savvides, H. Park, and M. B. Srivastava. “The n-hop multilateration primitive for node localization problems”. In: *Proceedings of Mobile Network Applications*. 2003, pp. 443–451.
- [39] A. Savvides et al. “Localization in sensor networks”. In: Norwell, MA, USA, 2004, pp. 327–349.
- [40] M. Segura, V. Mut, and C. Sisterna. “Ultra wideband Indoor Navigation System”. In: *IET Radar, Sonar and Navigation*. Vol. 6. 2012, pp. 402 –411.
- [41] Pankaj Sharma, Sivanand Krishnan, and Zhang Guoping. “A multi-cell UWB-IR localization system for robot navigation”. In: *Proceedings of IEEE Radio and Wireless Symposium*. 2008, pp. 402 –411.
- [42] Mark Sullivan. *A brief history of GPS*. URL: <http://www.pcworld.com/article/2000276/a-brief-history-of-gps.html>.
- [43] Jeremy G. VanAntwerp and Richard D. Braatz. “A tutorial on linear and bilinear matrix inequalities”. In: (2000), pp. 363 –385.
- [44] Xuyu Wang, Lingjun Gao, and Shiwen Mao. “PhaseFi: Phase Fingerprinting for Indoor Localization with a Deep Learning Approach”. In: *Proceedings of IEEE Global Communications Conference (GLOBECOM)*. 2015, pp. 1–6.
- [45] Xuyu Wang et al. “CSI-based Fingerprinting for Indoor Localization: A Deep Learning Approach”. In: *Proceedings of IEEE Transactions on Vehicular Technology*. 2016.
- [46] Xuyu Wang et al. “DeepFi: Deep learning for indoor fingerprinting using channel state information”. In: *Proceedings of IEEE Wireless Communications and Networking Conference (WCNC)*. 2015, pp. 1666 –1671.
- [47] Xuyu Wang et al. “Mobility improves LMI-based cooperative indoor localization”. In: *Proceedings of IEEE Wireless Communications and Networking Conference (WCNC)*. 2015, pp. 2215 –2220.

- [48] R. Want et al. “The active badge location system”. In: *Proceedings of ACM Transactions on Information Systems*. 1992, pp. 91–102.
- [49] Stijn Wielandt et al. “Performance Simulations of a 2.4 GHz Indoor Angle of Arrival System for Multipath Components”. In: *Proceedings of International Conference on Indoor Positioning and Indoor Navigation(IPIN)*. 2015, pp. 1–8.
- [50] Wikipedia. *Multilateration*. URL: <https://en.wikipedia.org/wiki/Multilateration>.
- [51] Wikipedia. *Round-trip Delay Time*. URL: https://en.wikipedia.org/wiki/Round-trip_delay_time.
- [52] Wikipedia. *Wireless Ad Hoc Network*. URL: https://en.wikipedia.org/wiki/Wireless_ad_hoc_network#Protocol_stack.
- [53] Wikipedia. *Wireless Sensor Network*. URL: https://en.wikipedia.org/wiki/Wireless_sensor_network.
- [54] Rong-Hou Wu et al. “Study of characteristics of RSSI signal”. In: *Proceedings of IEEE International Conference on Industrial Technology*. 2008, pp. 1–3.
- [55] Wang Xue, Song Shu Zhong, and Li Meng. “Design of Personnel Position System of Mine Based on The Average Of RSSI”. In: *Proceedings of IEEE International Conference on Automation and Logistics*. 2012, pp. 239–242.
- [56] Ting Yang, Qing Yang, and Alvin Lim. “Driver Layer Approach to Time-of-Arrival Ranging in IEEE 802.11g Networks”. In: *Proc. of the IEEE Consumer Communications and Networking Conference(CCNC)*. Las Vegas, Nevada, USA, 2012.
- [57] G. Zanca et al. “Experimental comparison of RSSI-based localization algorithms for indoor wireless sensor networks”. In: Glasgow, Scotland, 2008, pp. 1–5.
- [58] Yan Zi-Zong. “Schur Complements and Determinant Inequalities”. In: *Journal of Mathematical Inequalities* (2009), pp. 161–167.

- [59] Francesco Zorzi et al. “Opportunistic Localization Scheme Based on Linear Matrix Inequality”. In: *Proc. of the 6th IEEE International Symposium on Intelligent Signal Processing*. Budapest, Hungary, 2009, pp. 247–252.
- [60] L. Zwirello et al. “Sensor data fusion in UWB-supported inertial navigation systems for indoor navigation”. In: *Proceedings of IEEE Robotics and Automation*. 2013, pp. 3154–3159.